nature ecology & evolution

ARTICLES

https://doi.org/10.1038/s41559-022-01697-z

Innate immune pathways act synergistically to constrain RNA virus evolution in *Drosophila melanogaster*

Vanesa Mongelli[1], Sebastian Lequime[2], Athanasios Kousathanas[3], Valérie Gausson[1], Hervé Blanc[1], Jared Nigg[1], Lluis Quintana-Murci[3,4], Santiago F. Elena[5,6] ✉ and Maria-Carla Saleh[1] ✉

Host–pathogen interactions impose recurrent selective pressures that lead to constant adaptation and counter-adaptation in both competing species. Here, we sought to study this evolutionary arms-race and assessed the impact of the innate immune system on viral population diversity and evolution, using *Drosophila melanogaster* as model host and its natural pathogen *Drosophila* C virus (DCV). We isogenized eight fly genotypes generating animals defective for RNAi, Imd and Toll innate immune pathways as well as pathogen-sensing and gut renewal pathways. Wild-type or mutant flies were then orally infected with DCV and the virus was serially passaged ten times via reinfection in naive flies. Viral population diversity was studied after each viral passage by high-throughput sequencing and infection phenotypes were assessed at the beginning and at the end of the evolution experiment. We found that the absence of any of the various immune pathways studied increased viral genetic diversity while attenuating virulence. Strikingly, these effects were observed in a range of host factors described as having mainly antiviral or antibacterial functions. Together, our results indicate that the innate immune system as a whole and not specific antiviral defence pathways in isolation, generally constrains viral diversity and evolution.

Interaction between hosts and pathogens trigger defence and counter-defence mechanisms that often result in reciprocal adaptation and co-evolution of both organisms[1]. Empirical evidence of such arms-races involving both species can be drawn from genome-wide analysis of hosts and pathogens and in experimental evolution settings. For example, evolutionary analysis of mammalian genomes has revealed evidence of host–virus co-evolution between different retroviruses and antiviral factors[2,3] and, in plants, host resistance genes and virulence genes encoded by pathogens have been found to co-evolve[4]. Likewise, between bacteria and their infecting bacteriophages, experimental co-evolution studies resulted in the occurrence of genetic variants in both a bacterial lipopolysaccharide synthesis gene and the phage tail fibre gene which binds to lipopolysaccharide during adsorption[5]. In nematodes and their pathogenic bacteria, the number of toxin-expressing plasmids varies during adaptation to the host[6].

In insects, analyses of sequences within and between *Drosophila* species have shown evidence of adaptive evolution in immunity-related genes[7–10]. In a study that deep-sequenced small interfering RNAs (siRNAs) from mosquitoes infected with West Nile virus, it was found that the regions of the viral genome more intensively targeted by RNA interference (RNAi) contained a higher number of mutations than genomic regions less affected by this pathway, suggesting that this antiviral defence mechanism imposes a selective pressure on the viral population[11]. Similar observations on the selective pressure imposed by the RNAi pathway on viral evolution have been made in plant- and human-infecting viruses[12–16]. *Drosophila melanogaster* is a well-studied insect model to decipher virus–host interactions and therefore the impact of host antiviral immunity on viral diversity and evolution. Different *Drosophila* immune pathways and mechanisms are involved in antiviral defence[17,18]. As is the case for all invertebrates, defence against pathogens in *Drosophila* relies on innate immunity, which constitutes the first and only defence against microbes. Innate immunity is characterized by the recognition of pathogen-derived molecules, called pathogen-associated molecular patterns (PAMPs), by host-encoded receptors (pathogen-recognition receptors, PRRs), which leads to a rapid defence response.

The RNAi mechanism is known to play a central role in *Drosophila* antiviral defence, mainly through the action of the siRNA pathway[19–22]. Antiviral RNAi is triggered by virtually all insect-infecting viruses, resulting in targeting of the viral genome in a sequence-specific manner to control infection. Several other pathways have antiviral properties in flies but their roles against viruses seem to be virus specific. The Toll and Imd (immune deficiency) pathways, originally described to be involved in antibacterial and antifungal responses, have been shown to play a role in antiviral defence against *Drosophila* C virus (DCV), Cricket paralysis virus (CrPV), *Drosophila* X virus, Nora virus and Flock house virus[23–26]. The Janus kinase signal transducers and activators of transcription (JAK-STAT) pathway can be activated on DCV or CrPV infection in flies, triggering the expression of antiviral factors[27,28].

DCV, a positive-sense single-stranded RNA virus from the genus *Cripavirus* within the Dicistrioviridae family and Picornavirales order[29], is a well-characterized natural pathogen of the fruit fly that can be found in laboratory and wild populations[30]. As for many other *Drosophila*-infecting viruses, defence against DCV depends on the joint action of different innate immune pathways and mechanisms.

[1]Viruses and RNA Interference Unit, Institut Pasteur, CNRS, Paris, France. [2]Cluster of Microbial Ecology, Groningen Institute for Evolutionary Life Sciences, University of Groningen, Groningen, the Netherlands. [3]Human Evolutionary Genetic Unit, Institut Pasteur, CNRS, Paris, France. [4]Human Genomics and Evolution, Collège de France, Paris, France. [5]Instituto de Biología Integrativa de Sistemas (CSIC—Universitat de València), València, Spain. [6]The Santa Fe Institute, Santa Fe, NM, USA. ✉e-mail: santiago.elena@csic.es; carla.saleh@pasteur.fr

RNAi, Toll and Imd pathways, but also the protein encoded by the gene *Vago*, play a role in the defence against this virus[20,24–27,31–33]. DCV is thought to be naturally acquired by ingestion[30,34,35]. For orally acquired pathogens, the digestive tract, and the gut in particular, represents the first host defence barrier. Despite many studies using oral bacterial infections[36], the role of gut-specific antiviral responses in *Drosophila* is not fully understood. Responses triggered against bacterial pathogens in the gut include the production of reactive oxygen species and antimicrobial peptides, as well as tissue repair and regeneration mechanisms[37]. Furthermore, the maintenance of gut homoeostasis after tissue damage caused by pathogenic bacteria relies on the activity of JAK-STAT and epidermal growth factor receptor (EGFR) pathways, amongst others[37–39]. In the hallmark of viral infections, a role of the Imd and extracellular-signal-regulated kinase (ERK) pathways in the antiviral response in the gut has been suggested[24,40]. It is important to note that, like many other RNA viruses with error-prone polymerases and fast replication kinetics, DCV exists as large populations composed of a cloud of genetically related mutant variants known as viral quasi-species or mutant swarms[41]. Viral mutant swarms constitute a dynamic repertoire of genetic and phenotypic variability that renders great adaptability.

In this work, we leveraged the vast knowledge on antiviral mechanisms, the extensive genetic tool-box available for *D. melanogaster*, the intrinsic variability of the DCV mutant swarm and the great depth power of next-generation sequencing (NGS) to study the impact of innate immune pathways on viral diversity and evolution. We aimed to determine not only if each pathway has a specific impact on the selective pressure imposed on DCV mutant swarm but also their relative impact. In addition, we investigated possible links between selected viral variants (viral function) and specific defence mechanisms. Our results with infections in flies defective for several immune pathways show that the host genotype has an impact on viral genetic diversity regardless of the immune pathway being affected and this is accompanied by an attenuation of the virulence along evolutionary passages. We also describe complex mutation dynamics, with several examples of clonal interference in which increases in frequency of adaptive mutations have been displaced by other mutations of stronger effect that arose in different genetic backgrounds. Overall, our results highlight that innate immune pathways constrain RNA virus evolution and further demonstrate that antiviral responses in *Drosophila* are probably polygenic.

Results

Production of fly mutant lines for innate immune pathways. To determine the impact of the innate immune system on virus population diversity and evolution, we selected fly lines with impaired function in genes belonging to most of the *Drosophila* innate immune pathways: RNAi, Toll and Imd. We selected genes encoding for proteins involved both upstream and downstream of the immune pathways, such as receptors or ligands that trigger the immune response and effectors of the response (Fig. 1a): for the RNAi pathway, Dicer 2 (Dcr-2) and Argonaute 2 (Ago-2); for the Toll pathway, the ligand of Toll receptor Spätzle (spz) and the NF-κB transcription factor dorsal-related immunity factor (Dif); for the Imd pathway, the NF-κB transcription factor Relish (Rel). We also added to the study the host factor Vago, that is upregulated during viral infections in a Dicer 2-dependent manner. Because DCV is orally acquired, and to explore the impact of gut homoeostasis on the antiviral response, a mutant line for epidermal growth factor receptor (*Egfr*), a gene involved in gut epithelium renewal, was also included in our panel. With the exception of *Egfr* and *Dif*, all of the selected genes were previously described to play an antiviral role against DCV infection[19–21,23–25]. It is important to mention that, in contrast to the RNAi antiviral mechanism that relies on the direct interaction between the components of the RNAi pathway and the viral genome, the molecular mechanisms underlying the antiviral responses mediated by Toll, Imd and Vago in *Drosophila* remain largely unknown.

To reduce genetic variation due to differences in genetic background, mutant flies were isogenized before beginning viral evolution experiments. Homozygous loss-of-function lines for *Dcr-2* (*Dcr-2*^{L811fsX} and *Dcr-2*^{R416X}), *Ago-2* (*Ago-2*^{414}), *spz* (*spz*^{2}), *Dif* (*Dif*^{1}), *Rel* (*Rel*^{E20}) and *Vago* (*Vago*$^{\Delta M10}$) and a hypomorphic mutant line for *Egfr* (*Egfr*^{t1}) were produced in the same genetic background by crossing parental lines at least ten times to *w*^{1118} flies. Infection phenotypes of the newly produced fly lines were characterized by following their survival after inoculation with DCV by intrathoracic injection (Supplementary Fig. 1a). As previously described, *Dcr-2*$^{L811fsX/L811fsX}$, *Dcr-2*$^{R416X/R416X}$ and *Ago-2*$^{414/414}$ mutants infected with DCV died faster than *w*^{1118} flies[20,21], as well as *Vago*$^{\Delta M10/\Delta M10}$ mutants[33]. Toll pathway mutants *spz*$^{2/2}$ and *Dif*$^{1/1}$ and Imd pathway mutant *Rel*$^{E20/E20}$ were less sensitive to DCV infection than *w*^{1118} flies as they died later than *w*^{1118} flies (Supplementary Fig. 1a); however, these mutants maintained the previously observed increased susceptibility to infection by Gram-positive and Gram-negative bacteria, respectively (Supplementary Fig. 1b,c). No difference in virus-induced mortality was found between *w*^{1118} and *Egfr*$^{t1/t1}$ mutant flies (Supplementary Fig. 1a). This set of isogenic mutant flies with contrasting phenotypes to DCV infection provided us with the host model system to perform the viral evolution experiment.

Experimental DCV evolution. To study the impact of innate immune pathways on virus population diversity and evolution, DCV from a viral stock was serially passaged (P1 to P10) in *w*^{1118} flies and in the isogenic innate immune-deficient fly lines (Fig. 1a,b). DCV population diversity was studied after each passage by NGS and DCV virulence was analysed at the beginning and at the end of the evolution experiment.

To follow viral infection during the course of the experiment, viral load ($TCID_{50}$) was determined by end-point dilution and prevalence (percentage of flies positive for $TCID_{50}$) was calculated for all passages in individual flies from DCV-contaminated cages. We found that for most fly genotypes and for both biological replicates, DCV infection prevailed along the ten viral passages (Extended Data Fig. 1a,b). When considering viral loads along passages, only *w*^{1118}, *Ago-2*$^{414/414}$ and *Rel*$^{E20/E20}$ fly lines displayed significant temporal dispersion (Durbin–Watson test for outliers <1.5), consistent among both biological replicates, while viral load in the other fly genotypes remained relatively stable (Durbin–Watson test in the range 1.5–2.5) for at least one of the biological replicates (Extended Data Fig. 1b). The negative strand of the DCV genome was detected in P10 in all genotypes and biological replicates, confirming that active viral replication occurred for the duration of the evolution experiment (Extended Data Fig. 1c). Whether remnants of non-replicating virus remained in the fly surface was not assessed. Of note, the DCV stock was experimentally introduced to the system only once, to start the P1.

To assess the impact that fly genotype, biological replicate and viral passage has on viral loads, the log-transformed $TCID_{50}$ values from each fly genotype (Extended Data Fig. 1d) were fitted to the generalized linear model (GLM) described in Methods. In short, the model incorporates fly genotype and experimental block as orthogonal factors and passage as covariable. Highly significant differences were observed in viral load among fly genotypes (test of the intercept: $\chi^2 = 146.734$, 8 d.f., $P < 0.001$) that were of very large magnitude ($\eta_P^2 = 84.85\%$), thus confirming that DCV load strongly varied among host genotypes. A significant effect was also observed for the viral passages (test of the covariable: $\chi^2 = 5.075$, 1 d.f., $P = 0.024$), indicating overall differences in viral accumulation among passages, although the magnitude of this effect was rather small ($\eta_P^2 = 0.28\%$). Regarding second-order interactions among factors and the

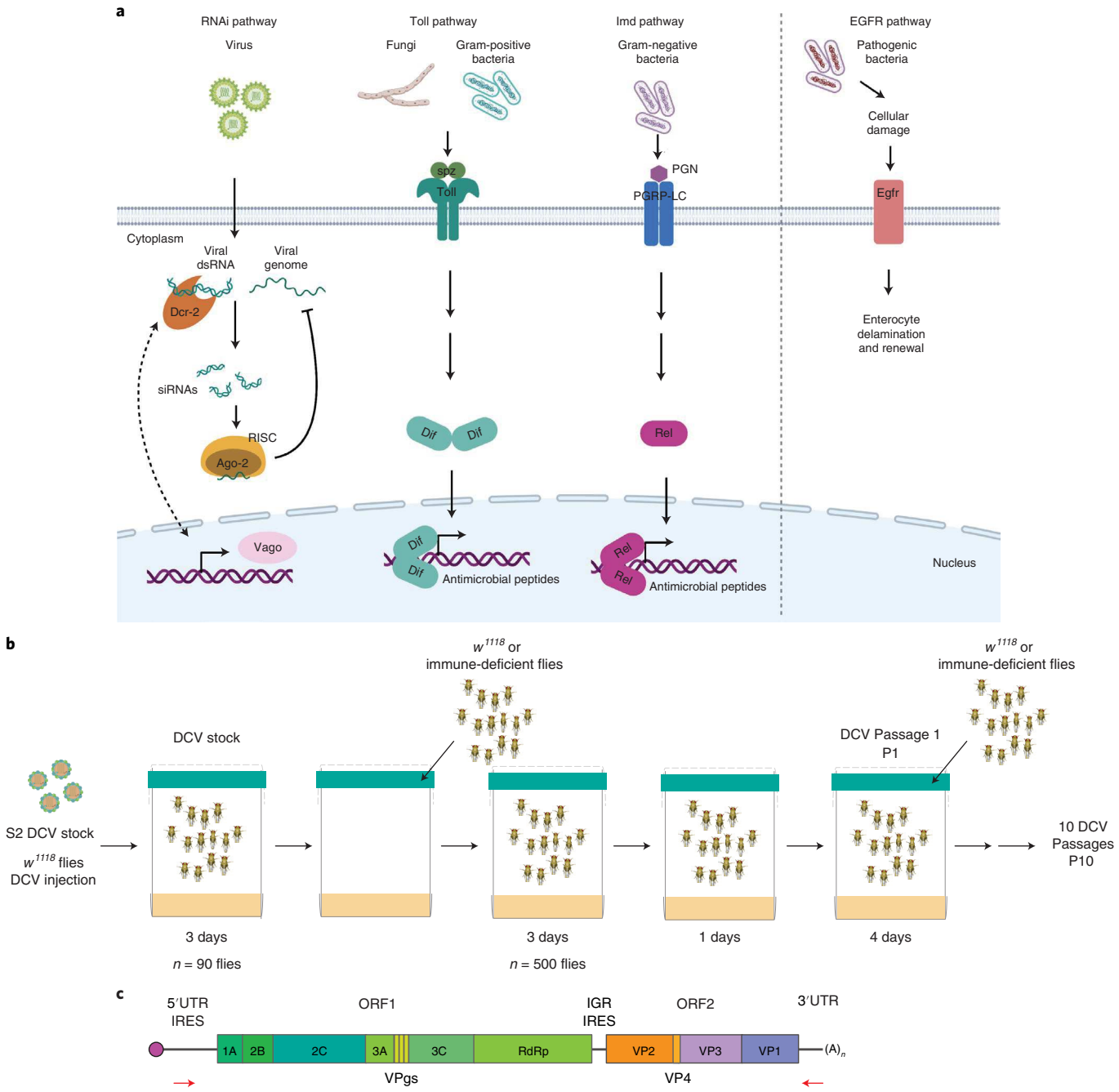

Fig. 1 | Experimental design. a, Simplified scheme of *D. melanogaster* immune pathways. The siRNA pathway is triggered by virus-derived double-stranded RNA (dsRNA), recognized by Dcr-2 and cleaved into viral siRNAs, which guide the recognition and cleavage of viral RNA by Ago-2 controlling virus infection. The Toll pathway is activated when spz binds to the Toll receptor, leading to the activation of NF-κB transcription factors (for example, Dif). The Imd pathway is triggered after the recognition of microbial peptidoglycans (PGN) by PGRP-LC, ultimately leading to the activation of Rel. Toll and Imd pathways induce the expression of antimicrobial peptides to control infection. The expression of Vago is induced after infection with DCV. The EGFR pathway is triggered in the gut after bacterial damage and leads to delamination of enterocytes and renewal. Created with BioRender.com. **b**, Scheme of the DCV evolution experiment. To produce the DCV stock, w^{1118} female flies were injected with DCV from a stock produced in S2 *Drosophila* cells (S2 DCV stock), placed in cages containing fresh *Drosophila* medium, left for 3 days and then removed to place in these DCV-contaminated cages $n = 500$ w^{1118} or immune-deficient males and females. Flies were fed ad libitum for 3 days, moved to a clean cage for 1 day and further placed into a new clean cage for 4 days, when they were harvested (DCV passage 1, P1). A new group of 500 flies was placed in contaminated cages. This procedure was repeated ten times (ten DCV passages, P1 to P10) and replicated twice (biological replicates BR1 and BR2). For each passage and fly genotype, high-throughput sequencing and viral stocks for phenotypic characterization were obtained. **c**, Scheme of DCV genome and the location of primers used to amplify the genome. The viral genome is composed of single-stranded positive-sense RNA and contains two open reading frames (ORFs). ORF1 encodes for the non-structural viral proteins: 1A, viral silencing suppressor; 2C, RNA helicase; VPg, viral genome-linked protein; 3C, protease; RdRp, RNA-dependent RNA polymerase; 2B and 3A, assembly of the viral replication complex. ORF2 encodes for DCV structural proteins VP1 to VP4, which constitute the viral capsid.

covariable, a significant interaction exists between fly genotype and experimental block ($\chi^2 = 27.082$, 8 d.f., $P < 0.001$) indicating that some of the differences observed in virus accumulation among host genotypes differed among biological replicates and between fly genotype and evolutionary passage ($\chi^2 = 52.511$, 8 d.f., $P < 0.001$). However, despite being statistically significant, these two effects were of very small magnitude ($\eta^2_P = 2.88\%$ and $\eta^2_P = 1.49\%$, respectively), casting doubts about their biological irrelevant. Likewise, the third-order interaction was statistically significant ($\chi^2 = 86.023$, 8 d.f., $P < 0.001$), suggesting that the differences in viral load among experimental blocks observed for a particular host genotype also depended on the evolutionary passages, although once again the effect could be considered as minor ($\eta^2_P = 1.49\%$). Next, we evaluated whether differences exist in viral load between immune-competent (w^{1118}) and the different mutant fly genotypes. In all eight cases, DCV accumulated to significantly higher levels in the immune-deficient flies than in the wild-type flies ($P < 0.001$), with the smallest significant difference corresponding to viral populations replicating in $Rel^{E20/E20}$ and $Dif^{1/1}$ and the largest to those replicating in $Egfr^{1/t1}$ and $Dcr\text{-}2^{R416X/R416X}$ (Extended Data Fig. 1d).

Overall, these results show that in both immune-competent (w^{1118}) and immune-deficient flies, DCV oral infection was maintained along passages and confirm that mutant flies are more permissive to DCV infection.

Viral nucleotide diversity increases in the absence of a fully functional immune response. To look into the selective pressure imposed by the *Drosophila* innate immune pathways on DCV population variation and dynamics, we analysed virus genome diversity after each passage. Half of the population of infected flies was used to sequence the full-length DCV genome by NGS (Fig. 1b,c). The viral stocks used to start the experiment, S2 DCV stock and DCV stock, were also sequenced (Methods). Analysis of the NGS data was performed using the computational pipeline Viral Variance Analysis (ViVan)[42]. Sequence coverage was at least 8,000 reads per position on the genome. To determine the error rate of the sequencing procedure, including library preparation, four sequencing technical replicates of the S2 DCV stock were used (Supplementary Fig. 2). An allele frequency threshold of 0.0028 was used for all subsequent analyses based on variant detection and frequency correlation between technical replicates (Methods). We next calculated the site-averaged nucleotide diversity (π) on all polymorphic sites ($n = 1{,}869$) across the full-length viral genome and present in the full dataset (Fig. 2), with the aim of determining if the lack of activity of a given innate immune pathway had an impact on viral population genetic diversity, in terms of size of the viral mutant swarm.

First, we asked if there was any difference in DCV population diversity and dynamics between the different fly genotypes along the complete evolution experiment. To answer this question, we analysed if the host genotype, viral passages, biological replicate or the interactions between these factors had an impact on the evolution of viral population diversity, considering the full-length DCV genome, across all passages. We found that only the fly genotype had a statistically significant impact on π ($\chi^2 = 25.545$, 8 d.f., $P = 0.001$) (Table 1). We then compared the DCV population diversity present in each fly genotype to each other. We found that, except for viral diversity found in $Dcr\text{-}2^{L811fs/[L811fsX}$ and $Dif^{1/1}$ lines, for which no difference was found compared to π in w^{1118} flies ($P \geq 0.303$), DCV population diversity significantly differed from w^{1118} line in the rest of the innate immune mutants analysed ($P \leq 0.013$) (Supplementary Table 1). A post hoc Bonferroni test further sorted overlapping groups according to their increasing viral nucleotide diversity: group 1 (less diversity)—w^{1118}, $Dcr\text{-}2^{L811fs/[L811fsX}$ and $Dif^{1/1}$ fly lines; group 2—$Dif^{1/1}$, $Dcr\text{-}2^{L811fs/[L811fsX}$, $Rel^{E20/E20}$, $spz^{2/2}$ and $Dcr\text{-}2^{R416X/R416X}$ fly lines; group 3—$Dcr\text{-}2^{L811fs/[L811fsX}$, $Rel^{E20/E20}$, $spz^{2/2}$, $Dcr\text{-}2^{R416X/R416X}$ and $Ago\text{-}2^{414/414}$ fly lines; group 4 (more diversity)—containing $spz^{2/2}$, $Dcr\text{-}2^{R416X/R416X}$, $Ago\text{-}2^{414/414}$, $Egfr^{1/t1}$ and $Vago^{\Delta M10/\Delta M10}$ fly lines (Extended Data Fig. 2 and Supplementary Table 1).

Next, we wondered if the general differences observed in viral nucleotide diversity, between fly genotypes were associated with a particular viral genomic region (that is, if a determined viral function was affected during the evolution experiment) (Fig. 1c). Of note, the intergenic region internal ribosome entry site (IGR IRES) was not included in the analysis because its lack of genetic variation prevented us from determining its nucleotide diversity value. We found that the fly genotype had a statistically significant effect on the nucleotide diversity found in each DCV genomic region ($\chi^2 = 27.178$, 8 d.f., $P < 0.001$), which further differed between each specific viral genomic region ($\chi^2 = 11.698$, 8 d.f., $P = 0.008$). As a second-order interaction, an effect of the fly genotype and the biological replicate was found ($\chi^2 = 16.314$, 8 d.f., $P = 0.038$) (Table 1). Comparison of viral genetic diversity within the genomic regions allowed us to distinguish three main groups: group 1 (less diversity), 3′UTR; group 2, 5′UTR IRES; and group 3 (more diversity), ORF1 and ORF2 (Extended Data Fig. 2 and Supplementary Table 1).

Finally, we wondered if viral diversity evolved from the starting viral stock (DCV stock) in each fly genotype. The π present in P1, P5 and P10 was compared between fly genotypes and with the diversity present in the DCV stock. We found that pairwise comparisons of viral nucleotide diversity present in each fly genotype in P1, between each other and versus DCV stock, yield no statistically significant difference ($P = 1.000$) (Supplementary Table 1). In P5 viral diversity was reduced only in w^{1118} (group 1/2; $P = 0.026$ and $P = 0.032$) compared to the starting viral stock (Extended Data Fig. 2 and Supplementary Table 1). In P10, viral nucleotide diversity present in w^{1118} (group 1, $P = 0.032$ and $P = 0.041$), $spz^{2/2}$ (group 1, $P = 0.020$ and $P = 0.025$), $Dif^{1/1}$ (group 1, $P = 0.005$ and $P = 0.006$) and $Rel^{E20/E20}$ (group 1/2, $P = 0.046$) mutant flies was reduced when compared to DCV diversity from the DCV stock (Extended Data Fig. 2 and Supplementary Table 1).

Altogether, the results show that the absence of a fully functional immune system results in an increase of viral population diversity that remains constant along passages. They also show that the coding regions of the virus are more prone to accumulate variation than the non-coding regions where regulatory elements are present.

Viral population diversity derives from pre-existing standing genetic variation. Next, we examined if the levels of viral diversity observed in DCV populations from innate immune mutants compared to the w^{1118} line were accompanied with the fixation of particular genetic changes in the mutant swarms and whether (1) these changes can be associated with fitness effects, (2) potentially adaptive mutations arose in response to particular immune responses. To do so, we estimated the selection coefficients for each single nucleotide polymorphism (SNP) using their variation in frequency across evolutionary time (Fig. 3 and Extended Data Fig. 3), using a classic population genetics approach[43] (Table 2). Thirty-six SNPs yielded significant estimates of selection coefficients (this number reduces to ten if a stricter false discovery rate (FDR) correction is applied; Table 2). Twenty-one of them were already detected in the ancestral S2 DCV stock, hence a maximum of 15 new SNPs might have arisen during the evolution experiment. Estimated selection coefficients for all these SNPs ranged between −0.304 per passage (synonymous mutation RdRp/C5713U) and 1.204 per passage (VP2/G6311C non-synonymous change R16P), with a median value of 0.286 per passage (interquartile rank = 0.265). Nine mutations were observed in more than one lineage (range 2–7 lineages), with synonymous mutations VP3/U7824C appearing in seven lineages of six different host genotypes and mutation 5′UTR/A280U in five lineages of five host genotypes (Table 2). These nine SNPs were all present in the S2 DCV stock. Indeed, the frequency of SNPs among evolving lineages is significantly correlated with their frequency in the ancestral

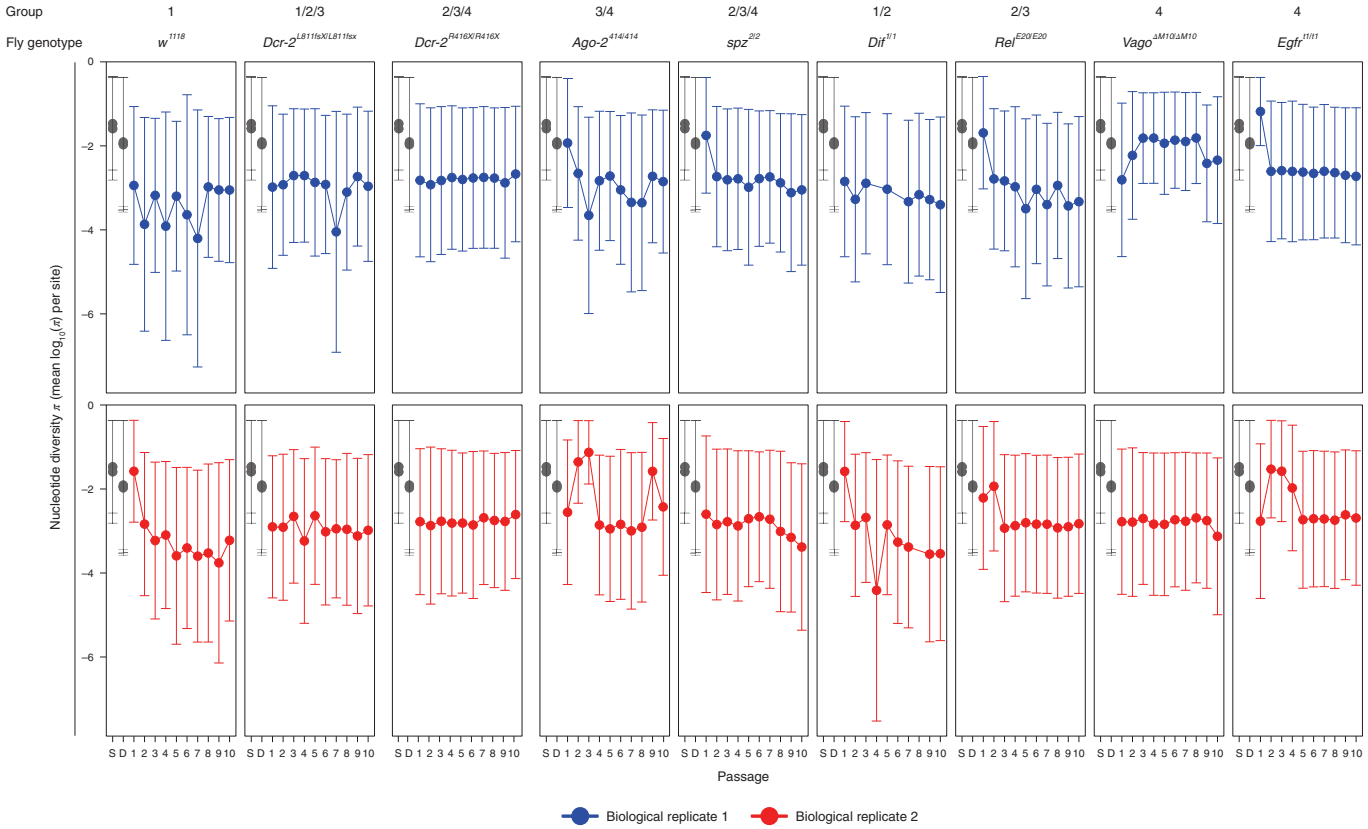

Fig. 2 | Viral nucleotide diversity differently evolves in each host genotype. Trajectory of the site-averaged nucleotide diversity (π) on all polymorphic sites ($n = 1{,}869$) across the full-length DCV genome found for each fly genotype and in each biological replicate of the evolution experiment. Group: DCV population diversity found in each fly genotype was pairwise compared and grouped by similarity after a Bonferroni post hoc test (Table 1 and Supplementary Table 1). S, S2 DCV stock; D, DCV stock, in grey.

S2 DCV stock (Pearson's $r = 0.401$, 36 d.f., $P = 0.013$) but not with their measured fitness effect ($r = -0.091$, 36 d.f., $P = 0.588$).

An interesting question is whether the fitness effects associated with each of these nine SNPs were the same across all genotypes or, conversely, whether fitness effects were host genotype-dependent. To test this hypothesis, we performed one-way analysis of variance (ANOVA) tests comparing fitness effects (Table 2) across the corresponding host genotypes. In all cases, significant differences were observed ($F \geq 15.637$ and $P \leq 0.001$ and $\geq 93.99\%$ of total observed variance in fitness effects explained by true genetic differences among host genotypes), supporting the notion that fitness effects are indeed host genotype-dependent. A pertinent example is the case of the synonymous mutation VP3/U7824C, which was the most prevalent mutation ($F_{6,45} = 158.862$, $P < 0.001$, 99.37% of genetic variance). In this case, a post hoc Bonferroni test shows that host genotypes can be classified into three groups according to the fitness effect of this SNP. In genotypes *Dcr-2*$^{R416X/R416X}$ and *Rel*$^{E20/E20}$, the mutation has a deleterious effect (on average, −0.2260 per passage); in genotypes *Egfr*$^{t1/t1}$ and *Vago*$^{\Delta M10/\Delta M10}$, the mutation is moderately beneficial (on average, 0.1257 per passage); and in genotypes *w*^{1118} and *Ago-2*$^{414/414}$, the mutation had a strong beneficial effect (on average, 0.502 per passage).

As shown in Fig. 3 and Extended Data Fig. 3a, some SNPs show a strong parallelism in their temporal dynamics, suggesting that they might be linked into haplotypes. This is particularly relevant for mutations shown in Table 2. To test this possibility, we computed all pairwise Pearson correlation coefficients between mutation frequencies along evolutionary time. The results of these analyses are shown in Extended Data Fig. 3b–k as heatmaps. Again, as an illustrative example, we discuss here the case of the viral population BR2 evolved in *Ago-2*$^{414/414}$ (Extended Data Fig. 3d). Synonymous mutations VP3/U7824C and VP1/C8424U and non-synonymous mutation VP1/C8227U (H655Y) are all linked into the same haplotype ($r \geq 0.998$, $P < 0.001$). Since these three mutations already existed in the S2 DCV stock, it is conceivable that the haplotype already existed and has been selected as a unit. Indeed, the fitness effects estimated for these three mutations are indistinguishable (one-way ANOVA: $F_{2,22} = 1.781$, $P = 0.192$; average fitness effect 0.590 ± 0.032 per passage), thus suggesting that the estimated value corresponds to the haplotype as a unit. The absence of this haplotype in *Ago-2*$^{414/414}$ BR1 suggests that it was lost during the transmission bottleneck from S2 cells to flies. Interestingly, mutations VP1/C8424U and VP1/C8227U appear also linked into the same haplotype in population BR2 evolved in *Dcr-2*$^{L811fsX/L811fsX}$ (Extended Data Fig. 3b). These two cases, as well as populations BR1 evolved in *Rel*$^{E20/E20}$, BR2 evolved in *spz*$^{2/2}$ and BR1 and BR2 evolved in *Vago*$^{\Delta M10/\Delta M10}$, illustrate some examples of haplotypes (Extended Data Fig. 3e,f,h,i). Other viral populations, especially those evolved in *Egfr*$^{t1/t1}$ flies, show much more complex patterns (Extended Data Fig. 3j,k) in which haplotypes change over time by acquiring de novo mutations.

When mapping the 36 SNPs found to have significant estimates of selection coefficients in the viral genome (Table 2 and Extended Data Fig. 4), we found that two mapped to the 5′UTR IRES, 12 to ORF1, one to the IGR IRES, 20 to ORF2 and one to the 3′UTR. Of the 12 mutations observed in ORF1, which encodes the non-structural proteins, four mapped to the 3C viral protease and

Table 1 | Analysis of the impact of each experimental variable on the evolution of DCV nucleotide diversity (mean $\log_{10}(\pi)$ per site)

	Experimental variable	χ^2	d.f.	*P*	
Full-length DCV genome	BR	2.2528	1	0.1334	
	VP	1.6460	1	0.1995	
	FG	25.5447	8	0.0013	**
	(BR)×VP	0.0024	1	0.9606	
	(BR)×FG	14.2963	8	0.0744	
	VP×FG	12.1679	8	0.1439	
	(BR)×VP×FG	10.4253	8	0.2364	
Each DCV genomic region	BR	1.2107	1	0.2712	
	VP	2.3528	1	0.1251	
	FG	27.1779	8	0.0007	***
	GR	11.6982	3	0.0085	**
	(BR)×VP	0.0001	1	0.9931	
	(BR)×FG	16.3143	8	0.0381	*
	VP×FG	8.3498	8	0.4000	
	(BR)×GR	0.7452	3	0.8625	
	VP×GR	0.9130	3	0.8223	
	FG×GR	24.0586	24	0.4583	
	(BR)×VP×FG	12.8802	8	0.1160	
	(BR)×VP×GR	0.1274	3	0.9884	
	(BR)×FG×GR	24.4811	24	0.4344	
	VP×FG×GR	10.5776	24	0.9917	
	(BR)×VP×FG×GR	28.3112	24	0.2471	

The site-averaged nucleotide diversity (π) on all polymorphic sites ($n=1{,}869$) across the full-length viral genome was determined, the $\log_{10}$-transformed π values were fitted to the GLM and the impact of the variables determined by an analysis of deviance (type III tests). BR, biological replicate; VP, viral passage; FG, fly genotype, GR, genomic region. *$P \leq 0.1$, **$P \leq 0.01$, ***$P \leq 0.001$.

five to the RdRp. Only one of these mutations in the 3C viral protease was non-synonymous. Of the 20 mutations in ORF2, which encodes the viral structural proteins, eight mapped to VP2, five to VP3 and seven to VP1. These correspond to the three majors predicted DCV capsid proteins.

Taken together, these results show that viral population diversity over these ten in vivo passages mainly derived from pre-existing standing genetic variation in the ancestral DCV population. Furthermore, temporal dynamics of population diversity were linked to the fly genotype in which the virus evolved.

DCV virulence decreases along passages in the absence of immune pathways. Finally, we wondered if DCV virulence varied among each lineage in the different fly genotypes. Infectious DCV stocks were produced from viral passages P1 and P10 and from all fly genotypes. Because the viral evolution experiment was performed by DCV orofecal transmission, we first evaluated DCV virulence by feeding w^{1118} flies with DCV stocks derived from P1 or P10; survival was evaluated from each fly genotype. We found that only a small proportion of flies (5–20%) succumbed to DCV infection and no statistically significant differences in mortality were found between mock- and virus-infected flies, regardless of viral passage or fly genotype (Supplementary Fig. 3). This is in agreement with previously published works showing that DCV oral infections are cleared in w^{1118} flies[31]. We next decided to investigate the evolution of virulence by intrathoracic inoculation of DCV stocks. We found that w^{1118} flies were less sensitive to viral infection when inoculated with DCV stocks derived from P10 since their median survival time was longer than those inoculated with stocks from P1 for most DCV stock origins (Fig. 4a and Supplementary Table 2). Notable exceptions were DCV stocks from BR2 of $Vago^{\Delta M10/\Delta M10}$ mutant flies, for which w^{1118} flies were more sensitive to P10 than to P1 and stocks from BR1 of $spz^{2/2}$ and BR2 of $Egfr^{t1/t1}$ mutant flies, for which no difference in median survival time after infection with DCV between P1 and P10 was detected.

A fundamental question in evolutionary biology is the role that past evolutionary events may have in the outcome of evolution[44]. If ongoing evolution is strongly contingent with past evolutionary events, ancestral phenotypic differences should be retained to some extent, while if other evolutionary forces such as selection and stochastic events (mutation and genetic drift) dominate, then ancestral differences can be eroded and, in the extreme case, even fully removed. Here, we observed significant differences in the performance of the ancestral DCV across the eight host genotypes. To test whether these differences are still observable in the evolved population, we compared the median survival time (Fig. 4a and Supplementary Table 2) for DCV populations isolated at the beginning of the evolution experiment P1 and at the end P10 (Fig. 4b). Under the null hypothesis of strong historical contingency, it is expected that data will fit to a regression line of slope 1 and intercepting the ordinate axis at 0. However, if ancestral differences have been removed, data would fit significantly better to a regression line with a slope <1 and with an intercept >0 (ref. [44]). Figure 4b shows the data and their fit to the null hypothesis (solid black line) and the alternative hypothesis (dashed red line). A partial *F*-test shows that adding an intercept to the regression equation significantly improves the fit ($F_{1,16}=28.437$, $P<0.001$), thus supporting the notion that ancestral differences among host genotypes have been removed by the action of subsequent adaptation, that is, the fixation of beneficial mutations.

Discussion

In this work we aimed at determining the overall impact of innate immunity on viral evolution. On the basis of the arms-race hypothesis, we speculated that if a given host defence mechanism imposes a specific selective pressure on a particular pathogen function, the absence of this defence mechanism would result in the relaxation of the selective constraint, which would in turn be detectable in the pathogen at the genomic and phenotypic levels. We found that viral population diversity evolved differently according to each fly genotype; however, viral population diversity mostly derives from ancestral standing genetic variation (that is, few 'new' mutations were selected). Our results further confirm the polygenic nature of antiviral responses; there is not a specific, main immune defence mechanism against a particular virus but instead a repertoire of defence mechanisms that are triggered after infection and that might interact with each other.

Our results are compatible with a pervasive presence of clonal interference. In the absence of sexual reproduction, clonal interference is the process by which beneficial alleles originated in different clades within a population compete with each other, resulting in one of them reaching fixation. Subsequently, the outcompeted beneficial allele may appear in the new dominant genetic background and, assuming no negative epistasis among both loci, become fixed. As a consequence, beneficial mutations may fix sequentially, thus slowing down the rate of adaptation[45]. Given their large effective population size and high mutation rates, viral populations are expected to contain considerable amounts of potentially beneficial standing variation, making them prone to clonal interference. Indeed, it has

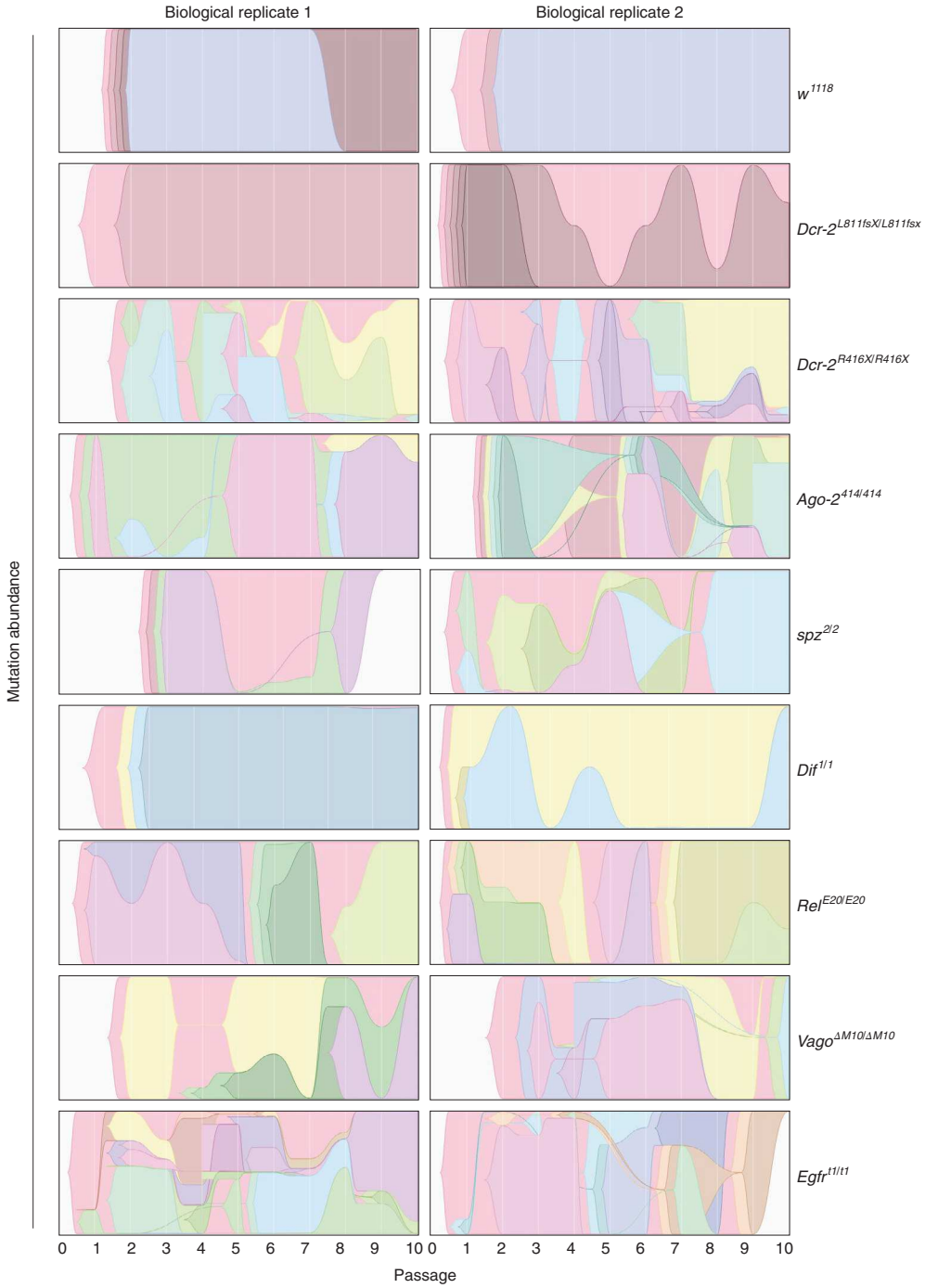

Fig. 3 | Trajectories of DCV variants across passages. Muller plots illustrating the dynamics of frequencies of SNPs along evolutionary time. Each colour represents the dynamics of a different SNP.

been previously shown to operate in experimental populations of vesicular stomatitis virus adapting to cell cultures[46,47], in bacteriophage ϕX174 populations adapting to harsh saline environments[48], in tobacco etch virus adapting to new plant host species[49], among HIV-1 escape variants within individual patients[50] and also at the epidemiological level among influenza A virus lineages diversifying antigenically[51]. In our own results, clonal interference can be observed in populations BR1 evolved in $Dcr\text{-}2^{L811fsX/L811fsX}$, BR1 evolved in $Ago\text{-}2^{414/414}$, BR1 evolved in $spz^{2/2}$, BR2 evolved in $Rel^{E20/E20}$ and BR2 evolved in $Vago^{\Delta M10/\Delta M10}$. All of these viral populations share similar patterns in which some beneficial allele (or haplotypes) rose in frequency, reached a peak at some intermediate passage, then declined in frequency and were finally outcompeted by a different beneficial mutation (or haplotype) that had lower initial frequency. For example, the non-synonymous mutation VP2/G6931A (A223T) appeared de novo in population BR1 evolved in $spz^{2/2}$ and outcompeted several mutations probably linked in a haplotype (Fig. 3). Tightly linked to clonal interference is the concept of leap-frogging[52], in which the beneficial mutation that ends up dominating the population is less genetically related to the previously dominant haplotype than to the common ancestor of both (Fig. 3). The VP2/G6931A mutation illustrates this case well, as it

Table 2 | Mutations for which significant estimates of fitness effects have been obtained

Fly genotype	Biological replicates	Mutation	Standing variation (frequency)	Selection coefficient per passage (± s.e.m.)	*P*
w^{1118}	1	VP2/G6311C R16P	Yes (0.0104)	1.2039 ± 0.2543	0.0418
w^{1118}	2	VP3/U7824C	Yes (0.1457)	0.4780 ± 0.0617	<0.0001*
$Dcr\text{-}2^{L811fsX/L811fsX}$	1	-			
$Dcr\text{-}2^{L811fsX/L811fsX}$	2	RpRd/U5302C	No	0.3877 ± 0.0973	0.0073
		VP1/C8227U H655Y	Yes (0.0147)	0.3735 ± 0.1368	0.0258
		VP1/C8424U	Yes (0.0139)	0.3880 ± 0.1407	0.0248
$Dcr\text{-}2^{R416X/R416X}$	1	VP2/C6932U A223V	Yes (0.0084)	0.2135 ± 0.0169	<0.0001*
$Dcr\text{-}2^{R416X/R416X}$	2	VP2/G6379A A39T	Yes (0.0098)	0.2074 ± 0.0555	0.0057
		VP3/A7465G I401V	Yes (0.0088)	0.1185 ± 0.0338	0.0100
		VP3/U7824C	Yes (0.1457)	−0.2887 ± 0.0884	0.0309
$Ago\text{-}2^{414/414}$	1	-			
$Ago\text{-}2^{414/414}$	2	5′UTR/A280U	Yes (0.1176)	−0.1307 ± 0.0376	0.0084
		VP3/U7824C	Yes (0.1457)	0.5251 ± 0.1050	0.0024
		VP1/C8227U H655Y	Yes (0.0147)	0.6238 ± 0.1077	0.0007
		VP1/C8424U	Yes (0.0139)	0.6206 ± 0.1252	0.0026
$Spz^{2/2}$	1	5′UTR/A280U	Yes (0.1176)	−0.2092 ± 0.0735	0.0215
		VP2/G6931A A223T	No	0.5420 ± 0.1477	0.0105
$Spz^{2/2}$	2	2A/A1128C D110A	Yes (0.0041)	−0.0229 ± 0.0065	0.0246
		3C-Prot/A3787G	No	0.5238 ± 0.0757	0.0002*
		3C-Prot/G4394A V1199I	No	0.5982 ± 0.0764	0.0002*
		VP1/G8536A V758I	No	0.7038 ± 0.0915	0.0006*
		IGR/A6108G	Yes (0.0044)	0.4873 ± 0.0692	0.0002*
		VP3/G8090A R609H	Yes (0.0200)	0.4947 ± 0.0722	0.0001*
$Dif^{1/1}$	1	VP3/A7465G I401V	Yes (0.0088)	0.3213 ± 0.1173	0.0338
		VP3/G7956A	No	0.2000 ± 0.0335	0.0094
$Dif^{1/1}$	2	5′UTR/A280U	Yes (0.1176)	0.5157 ± 0.1289	0.0052
		VP1/U8629C S5058P	Yes (0.0898)	0.4864 ± 0.1175	0.0043
$Rel^{E20/E20}$	1	5′UTR/A280U	Yes (0.1176)	0.3430 ± 0.1017	0.0097
		RdRp/A5404G	Yes (0.0929)	0.3993 ± 0.1217	0.0135
		VP2/U6303A N13K	Yes (0.0037)	0.5724 ± 0.1409	0.0036
		VP3/U7824C	Yes (0.1457)	−0.2804 ± 0.0206	0.0467
$Rel^{E20/E20}$	2	5′UTR/A280U	Yes (0.1176)	−0.0917 ± 0.0277	0.0130
		2B/C1412U	Yes (0.1301)	0.4554 ± 0.0119	0.0166
		VP3/C7760A T499N	No	0.1340 ± 0.0195	0.0005
$Vago^{\Delta M10/\Delta M10}$	1	2B/C1412U	Yes (0.1301)	0.2386 ± 0.0549	0.0025
		3C-Prot/A3703G	No	0.2859 ± 0.0537	0.0031
		RdRp/U5188A	Yes (0.1325)	0.2869 ± 0.0705	0.0268
		VP2/C6932U A223V	Yes (0.0084)	0.1368 ± 0.0553	0.0426
		VP1/C8227U H655Y	Yes (0.0147)	0.1936 ± 0.0291	0.0002*
		VP1/C8424U	Yes (0.0139)	0.1915 ± 0.0283	0.0001*
		VP1/U8697C	No	0.2053 ± 0.0325	0.0002*
		3′UTR/U9163A	No	0.1473 ± 0.0622	0.0497
$Vago^{\Delta M10/\Delta M10}$	2	2C-Hel/G1756A	Yes (0.0059)	0.3467 ± 0.1293	0.0364
		VP2/A6300U E12D	No	0.3681 ± 0.1297	0.0470
		VP3/U7824C	Yes (0.1372)	0.1517 ± 0.0391	0.0060
$Egfr^{t1/t1}$	1	5′UTR/A280U	Yes (0.1176)	0.1394 ± 0.0364	0.0050

Continued

Table 2 | Mutations for which significant estimates of fitness effects have been obtained (continued)

Fly genotype	Biological replicates	Mutation	Standing variation (frequency)	Selection coefficient per passage (± s.e.m.)	*P*
		3C-Prot/U3643A	No	−0.2064 ± 0.0592	0.0399
		VP1/A8201G Q646R	Yes (0.0045)	0.3198 ± 0.0736	0.0225
		VP2/A6660U	No	−0.1906 ± 0.0641	0.0409
		VP2/G6868A V8162I	No	0.3302 ± 0.0389	0.0001
		VP3/A7465G I401V	Yes (0.0088)	−0.1053 ± 0.0359	0.0261
		VP3/U7824C	Yes (0.1457)	0.0997 ± 0.0410	0.0411
$Egfr^{t1/t1}$	2	5′UTR/A198G	No	0.1035 ± 0.0363	0.0246
		RdRp/U4810C	Yes (0.1152)	−0.2635 ± 0.0301	0.0128
		RdRp/C5713U	Yes (0.1148)	−0.3036 ± 0.0276	0.0082
		VP2/G6379A A39T	Yes (0.0082)	0.0630 ± 0.0254	0.0381
		VP3/U7824C	Yes (0.1457)	−0.1090 ± 0.0402	0.0421
		VP3/G8090A R609H	Yes (0.0200)	0.0764 ± 0.0289	0.0333
		VP1/U8250G H662Q	Yes (0.0201)	0.1734 ± 0.0326	0.0060

For each mutation, we indicate whether it already existed in the S2 DCV stock (and at which frequency) or arose during the evolution experiment. We also provide the estimated selection coefficient, its s.e.m. and statistical significance. Cases significant after FDR correction are marked with an asterisk.

appeared in a genetic background that was minoritarian rather than in the dominant one. Likewise, the mutation VP2/G6311C (R16P), observed in BR1 evolved in w^{1118} flies, appeared in a low-frequency genetic background different from the most abundant one in previous passages. Finally, the haplotype containing five different mutations observed in BR2 evolved in $spz^{2/2}$ became dominant in frequency after P6, outcompeting two other mutations that were dominating the population until then.

The existence and fixation of haplotypes along our evolution experiment deserves further discussion. Linked mutations generate three possible interference effects[53]. First, all mutations might contribute additively, or may be involved in positive epistasis, to the fitness of the haplotype as a whole, thus increasing its chances to become fixed. Second, hitchhiking and genetic draft may occur, by which deleterious or neutral alleles are driven to fixation along with a linked beneficial allele. Third, there may be background selection by which the spread of a beneficial allele is impeded, or at least delayed, owing to the presence of linked deleterious alleles. For instance, we can hypothesize that haplotype VP3/U7824C-VP1/C8227U-VP1/C8424U, which swept to fixation in population BR2 evolved in $Ago\text{-}2^{414/414}$, may represent a case of genetic draft: two synonymous mutations, potentially neutral, linked to a non-synonymous one that may be the actual target of selection. Yet, the lack of an infectious clone for DCV does not allow us to test this hypothesis.

Some of the mutations we found to be associated with positive selection coefficients were synonymous changes (Table 2). However, equating synonymous mutations with neutral mutations in compacted RNA genomes has proven to be misleading[54,55]. Selection operates at different levels of a virus's infection cycle and not all these levels necessarily depend on the amino acid sequence of encoded proteins. For instance, a lack of matching between virus and host codon usages would slowdown translational speed and efficiency[56]; mutations affecting the folding of regulatory secondary structures at non-coding regions would affect the interaction with host and viral factors and thus impact the expression of downstream genes (for example, mutations 5′UTR/A280U, IGR/A6108G and 3′UTR/U9163A all with significant fitness effects—Table 2)[57]; or evasion from antiviral RNAi defences by changing the most important relevant sites in the target of siRNAs[12,13].

It is interesting to observe that viral diversity in mutants for antiviral RNAi, whose mode of action relies on a direct interaction with the viral genome, did not display increased diversity when compared to mutants from the other immune pathways. One could expect that the release of the selective pressure that RNAi exerts on the virus genome may allow for the appearance of mutations in the viral suppressor of RNAi. Nonetheless, we did not observe such a change, possibly because the RNAi suppressor in DCV shares the first 99 amino acids of the RdRp[20,58] and mutations would affect polymerase activity. The antiviral action of the other immune pathways remains still unknown and may even be indirect; for example, the known roles of Imd, Toll and Egfr pathways in controlling fly microbiota[38,39] might possibly affect the prevalence of virus infections. In this regard, it is important to highlight that the diversity of DCV in the $Dif^{1/1}$ mutant (Toll pathway, already described not to have an impact on DCV defence[25]), was indistinguishable from w^{1118}, pointing to the specific—although uncharacterized—antiviral functions of the other immune pathways.

Another consideration when interpreting our results is the nature of the virus stock used. This virus stock has been maintained for years in *Drosophila* S2 cells. The observation that viral population diversity decreased along passages in w^{1118} flies, highlights the strength of the selective forces that constrain the virus from adapting to a new environment. During the successive passages, in the absence of a given immune response, the capacity of the virus to evolve will be determined by a combination of two factors: the adaptation to the new environment (constraining factor) and the lack

Fig. 4 | DCV virulence decreases in the absence of immune pathways. DCV infectious stocks were prepared from viral passages P1 and P10 and from each fly genotype. The w^{1118} flies were intrathoracically inoculated with ten $TCID_{50}$ units of each DCV stock and survival of the flies was measured daily. **a**, Survival curves shown in the figure are the combination of the two independent replicates, with three technical replicates each, of a total of at least $n = 98$ flies per treatment. Error bars indicate ± s.e.m.; NS, not significant. Survival curves were compared via log-rank (Mantel–Cox) tests. **b**, Test of the contribution of historical contingency evolved (P10) versus ancestral (P1) DCV virulence. The dashed red line represents the linear regression and the black line represents the expected relationship under the null hypothesis of ancestral differences in DCV virulence which are maintained after evolution despite noise introduced by random events (mutation and drift).

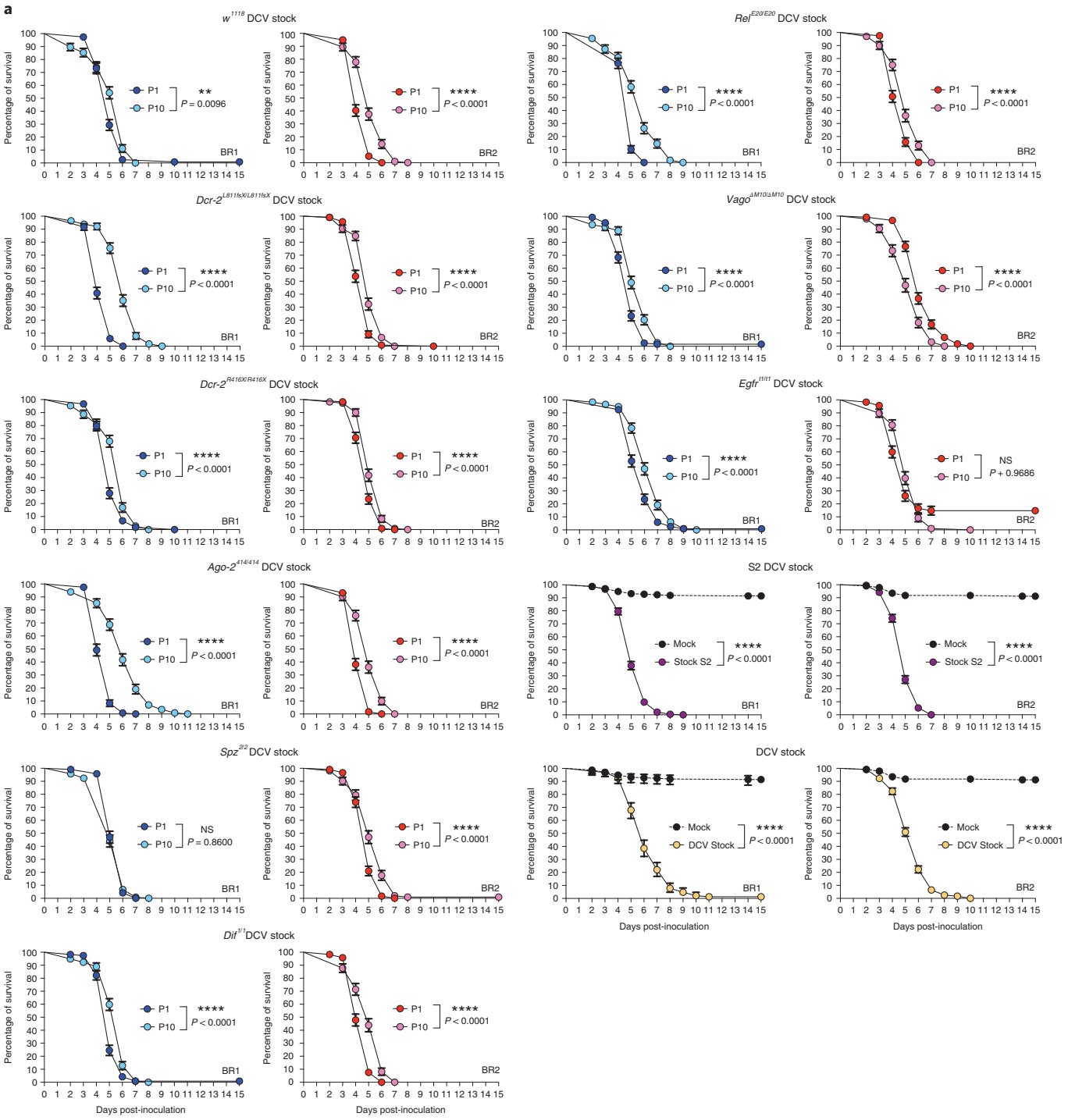
a
w1118 DCV stock
Rel E20/E20 DCV stock
Dcr-2 L811fsX/L811fsX DCV stock
Vago ΔM10/ΔM10 DCV stock
Dcr-2 R416X/R416X DCV stock
Egfr 1/1 DCV stock
Ago-2 414/414 DCV stock
S2 DCV stock
Spz 2/2 DCV stock
DCV stock
Dif 1/1 DCV stock
Percentage of survival
P1
P10
Mock
Stock S2
DCV Stock
** P = 0.0096
**** P < 0.0001
NS P = 0.8600
NS P + 0.9686
BR1
BR2
Days post-inoculation
b
Median survival flies infected with evolved virus
Median survival flies infected with ancestral virus
w1118
Dcr-2 L811fsX/L811fsx
Dcr-2 R416X/R416X
Ago-2 414/414
spz 2/2
Dif 1/1
Rel E20/E20
Vago ΔM10/ΔM10
Egfr 1/1
BR1
BR2

of immune response (relaxation factor). Because DCV replication is significantly increased in immune-deficient mutants, the potential for population diversification is higher. This effect is clearly observed in w^{1118} flies where the virus is 'only' adapting to the new environment and DCV populations evolved in w^{1118} flies show less variation than all other lineages. Future experimental evolution studies using viral stocks derived from flies, instead of cell cultures, are warranted to address this topic.

In a study published recently[59], Navarro et al. used *Arabidopsis thaliana* and turnip mosaic virus to carry out experimental virus evolution assays with a similar design to ours. In their work, the authors used plant mutants compromised in their antiviral response (more permissive to viral infection) or with an enhanced antiviral response (less permissive to viral infection) and allowed the virus to evolve for 12 passages. Similarly to what we found in the *D. melanogaster*–DCV system, the authors showed that viral population evolution dynamics, as well as viral loads, depend on host genotype. Interestingly, a reduction of ancestral genetic variation regardless of the immune pathway affected was also clearly observed, in agreement with our observations.

Taken together, our results point to the concerted action of the different immune pathways to limit viral evolution. Response to infection does not simply consist of activating immune pathways, it also encompasses a broad range of physiological consequences including metabolic adaptations, stress responses and tissue repair. Critically, on infection, the homoeostatic regulation of these pathways is altered. However, such alterations do not always result in increased disease severity and in fact can even lead to improved survival (or health) despite active virus replication.

Methods

Fly strains and husbandry. Flies were maintained on a standard cornmeal diet (Bloomington) at a constant temperature of 25 °C. All fly lines were cleaned of possible chronic infections (viruses and *Wolbachia*) as described previously[60]. The presence or absence of these chronic infections was determined by PCR with reverse transcription with specific primers for Nora virus, *Drosophila* A virus, DCV (NoraVfor ATGGCGCCAGTTAGTGCAGACCT, NoraVrev CCTGTTGTTCCAGTTGGGTTCGA, DAVfor AGAGTGGCTGTGAGGCAGAT, DAVrev GCCATCTGACAACAGCTTGA, DCVfor GTTGCCTTATCTGCTCTG, DCVrev CGCATAACCATGCTCTTCTG) and by PCR with specific primers for *Wolbachia* sp. (wspfor TGGTCCAATAAGTGATGAAGAAAC, wsprev AAAAAT TAAACGCTACTCCA and wspBfor TTTGCAAGTGAAACAGAAGG, wspBrev GCTTTGCTGGCAAAATGG).

Fly mutant lines $Dcr\text{-}2^{L811fsX}$ and $Dcr\text{-}2^{R416X}$ (ref. [61]), $Ago\text{-}2^{414}$ (ref. [62]), Spz^{2} (ref. [63]), Dif^{1} (ref. [64]), Rel^{E20} (ref. [65]), $Vago^{\Delta M10\,33}$ and $Egfr^{f1}$ (ref. [66]) were isogenized to w^{1118} fly line genetic background first by replacing the chromosomes not containing the mutation using balancer chromosomes and then by recombination by backcrossing at least ten times to w^{1118} line. The presence of the mutation was followed during and at the end of the backcrossing procedure by PCR and sequence analysis using specific primers (Dcr2811_3001for TTTGACCCATGACTTTGCGGT, Dcr2811_3294rev CCTTGCAGAGATGCCCCTGTT, Dcr2416_4341for GAT TGGCATTACCGTCCCGAA, Dcr2416_4670rev AGCGATTCCTGATGA GTCTTA, Ago2414_rev TTGTGGATGGCTGTTGTCTCG, Ago251B414_for AGAGTCCCCACTTGAATGGCC, Spz2_for GCCTTTGGCGCTTGCCTAATT, Spz2_rev GCTCCTGCAAAGGAATCGCTC, Dif1_for CTTGGCAATCTTCTC GCACAG, Dif1_rev ATCGTGGTCTCCTGTGTGACG, Rel_Ex4rev AGCTCTC CAGTTTGTGCCGAC, Rel-RD_5′UTRfor CTGGCGTTAGTTTCGGCGTTG, Vagod10_for TTGGCCAACGGAAAGGATGTG, Vagod10_rev TGCCACCGA TGATCAATGACA, Egfrt1_for CAAAGCTCGAACCGAAATTA, Egfrt1_rev CTTTCTTAACGTCCACATGA).

Virus production and titration. The S2 DCV stock used to start the experiment was prepared in S2 cells. Cells were maintained in Schneider culture medium and at 25 °C and observed daily. Cells were harvested when cytopathic effects were detected, then frozen at −80 °C, thawed on ice and centrifuged for 15 min at 15,000*g* at 4 °C. The supernatant was recovered, aliquoted and stored at −80 °C. Viral stocks were titred in S2 cells, determined using the end-point dilution method and expressed as 50% tissue culture infective dose ($TCID_{50}$)[67].

To produce the DCV stocks from passages P1 and P10 from the evolution experiment half of the population of flies infected with DCV from each fly genotype (~250 flies) was homogenized in 1× PBS, homogenates were frozen at −80 °C, then thawed on ice, centrifuged to discard the tissue debris, supernatant was recovered and filtered to discard bacteria contamination, then aliquoted and stored at −80 °C. Viral stocks were titred in S2 cells using the end-point dilution method and expressed as $TCID_{50}$.

Viral and bacterial infections and survival analysis. To characterize the isogenized fly lines, 4- to 5-day-old female flies were intrathoracically injected with a Nanoject II apparatus (Drummond Scientific) with 50 nl of the pathogen suspension. For DCV infections, a suspension of 10 $TCID_{50}$ units of DCV in 10 mM Tris buffer, pH 7 was used. An injection of the same volume of 10 mM Tris, pH 7 served as a mock-infected control. Infected flies were kept at 25 °C, transferred into fresh vials every 2 d and number of dead flies was scored daily. For bacterial infections, 50 nl of suspensions in 1× PBS buffer, pH 7, of optical density (OD) = 10 for *Enterococcus faecalis* and of OD = 200 for *Erwinia carotovora carotovora* 15 (Ecc15) were used. An injection of the same volume of 1× PBS buffer served as a mock-infected control. Flies infected with *E. faecalis* were kept at 25 °C and flies infected with Ecc15 were kept at 29 °C. Flies were transferred into fresh vials every 2 d and number of dead flies was scored daily.

Virus experimental evolution. To produce the starting DCV stock (DCV stock) 5–6-day-old w^{1118} female flies were intrathoracically injected with 100 $TCID_{50}$ of DCV from a stock produced in S2 *Drosophila* cells (S2 DCV stock) or mock infected. At 4 days post-inoculation, $n = 90$ DCV-infected flies (DCV stock) were placed in cages containing fresh medium, left for 3 days and then removed to place in this DCV- or mock-contaminated cages $n = 500$ 5–6-day-old wild-type or mutant flies (males and females). Flies were allowed to feed ad libitum for 3 days (oral inoculation period), then moved to a clean cage for 1 day and further placed into a new clean cage and left for 4 days, when they were harvested (P1). A new group of flies was then placed into the contaminated cages. This procedure was repeated ten times (ten DCV passages, P1 to P10) and replicated twice (biological replicates BR1 and BR2). The total amount of flies from each passage, fly genotype and biological replicate was collected and randomly divided in halves (~250 flies), one half was used to extract total RNA and produce the NGS libraries and the other half to produce viral stocks to evaluate DCV virulence.

Characterization of infection during passages. Individual flies from each passage were anesthetized and homogenized in 100 ml of 1× PBS buffer. The tubes containing the homogenates were centrifuged for 5 min at 15,000*g* at 4 °C to discard the tissue debris. The supernatant was recovered and used to determine viral load ($TCID_{50}$) by end-point dilution and prevalence (percentage of flies positive for $TCID_{50}$) for each fly genotype, viral passages and biological replicate.

For statistical analyses, $TCID_{50}$ data were transformed as $T = \log(TCID_{50} + 1)$ and then fitted to a GLM in which fly genotype (G) and BR (B) were treated as orthogonal factors. G was considered as a fixed-effects factor whereas B was considered as a random-effects factor. Evolutionary passage (P) was introduced in the model as a fixed-effects covariable. We also considered second- and third-order interactions between the two factors and the covariable. The model equation thus reads:

$$T_{ijk}(P) \sim \tau + P + G_i + B_j + (P \times G)_i + (P \times B)_j + (G \times B)_{ij} + (P \times G \times B)_{ij} + \varepsilon_{ijk}$$

Where $T_{ijk}(P)$ is the transformed $TCID_{50}$ observed for a particular titration assay k of BR j of fly genotype i, τ represents the grand mean value and ε_{ijk} stands for the error assumed to be Gaussian distributed at every P. The significance of each term in the model was evaluated using a likelihood ratio test that follows a χ^2 probability distribution. The magnitude of the effects was evaluated using the η_P^2 statistic (proportion of total variability in the traits vector attributable to each factor in the model; conventionally, values of $\eta_P^2 \geq 0.15$ are considered as large effects). These analyses were done using SPSS v.27 (IBM).

Detection of negative-strand DCV RNA by strand-specific RT–qPCR (ssRT–qPCR). To determine the amount of negative-strand DCV RNA present in the viral stocks produced from each fly genotype in P10, S2 DCV stock and DCV stock, total RNA was extracted from the DCV stocks produced from P10 (all fly genotypes, both biological replicates) and from the DCV stocks used to start the experiment. Strand-specific quantitative PCR with reverse transcription (ssRT–qPCR) was performed with these RNA samples essentially as described[35]. We used 800 ng of RNA to perform reverse transcription with SuperScript II reverse transcriptase (Invitrogen) according to the manufacturer's instructions, with the exception that primer annealing occurred at 70 °C and complementary DNA synthesis occurred at 50 °C for 30 min. Reverse transcription was performed using a forward primer containing a non-target tag sequence (DCV_tag_F: AATTCAAGCTCGTCTTCCTCGAGGCTGTGTTTGCGCGAAG) A standard curve was produced by reverse transcription of a tenfold dilution series (from 10^8 to 10^3 copies per reaction) of in vitro transcribed RNA corresponding to a portion of the full-length negative-strand DCV RNA. Following reverse transcription, cDNA was diluted 1:10 and used for qPCR with the Luminaris Colour HiGreen low ROX qPCR Master Mix (Thermo Scientific) according to the manufacturer's

instructions. A forward primer containing the non-target tag sequence (Tag_qPCR_F: AATTCAAGCTCGTCTTCCTCG) and a a DCV-specific reverse primer (DCV_qPCR_R: AATGGCAAGCGCACACAATTA) were used for qPCR.

RNA extraction, cDNA synthesis and NGS library production. To produce the NGS libraries from the evolution experiment, half of the total population of flies infected with DCV from each fly genotype, viral passage and biological replicates (~250 flies) was used. To produce the NGS libraries from the viral stock from S2 cells (S2 DCV stock), two different aliquots of the stocks were used. To produce the NGS libraries from the DCV stock (virus infecting w^{1118} female flies used to contaminate the cages to start the evolution experiment), half of the population of the infected flies (~800 flies: $n = 90$ flies per cage × 9 fly genotypes × 2 BR) was used. In all cases, total RNA was extracted using TRIzol reagent (Invitrogen) following the manufacturer's instructions and the final concentration was determined using a NanoDrop ND-1000 Spectrophotometer. Then 300 ng of total RNA were used to produce the cDNA using oligo(dT) as primers reverse transcription with the Maxima H Minus Reverse Transcriptase Kit (Thermo Fisher Scientific) according to manufacturer's instructions. The cDNA obtained served as template to amplify the full-length genome of DCV with specific primers (DCVfor ATATGTACACACGGCTTTTAGGT and DCVrev CAGTAAGCAGGAAAATTGCG) using Phusion High-Fidelity DNA polymerase Kit (Thermo Fisher Scientific) in the following conditions: initial denaturation at 98 °C for 30 s; 30 cycles of denaturation at 98 °C for 10 s, annealing at 55 °C for 30 s and extension at 72 °C for 5 min; and final extension at 72 °C for 10 min. For both S2 DCV stock and DCV stock, four different DCV PCR amplifications were done to produce a total of four technical replicates of the NGS libraries. The PCR products were gel purified using the NucleoSpin Gel and PCR Clean-up kit (Machery-Nagel) and their concentration was determined using a NanoDrop ND-1000 Spectrophotometer. A total 200 ng of the purified PCR product were fragmented into 200–300-nucleotides-long products using an LE220 ultrasonicator (Covaris) following the manufacturer's instructions. The obtained fragments were used to produce the NGS library using the NEBNext UltraII DNA Library Prep Kit for Illumina (New England BioLabs), according to manufacturer's instructions. The quality of the libraries was verified using a High Sensitivity DNA Chip (Agilent) and quantified using the Quant-iT DNA assay kit (Thermo Fisher Scientific). A 1 nM dilution of the libraries was used for the sequencing that was performed on a NextSeq sequencer (Illumina) with a NextSeq 500 Mid Output kit v.2 (Illumina) (151 cycles). Two of the four technical replicates for S2 DVC stock and DCV stock were included in each run.

Sequencing of DCV populations from $Dif^{1/1}$ mutant flies from P4 to P6 from BR1 and P8 from BR2 did not work.

Genetic diversity analyses. *Variant frequency threshold.* To determine the error rate of the sequencing procedure, including library preparation, four sequencing technical replicates from S2 DCV stock were used (Supplementary Fig. 3a). First, pairwise comparison was done to identify the variant frequency threshold above which at least 95% of the variants were detected in both considered replicates (highest detection threshold = 0.0028). All variants above detection threshold were then correlated between each technical replicate to ensure good correlation between reported frequency values: the Pearson correlation coefficient between the detected frequency for variants was $r \geq 0.982$ for all pairwise correlation ($P < 0.001$). The R packages used for these analysis were described elsewhere[68–71].

Nucleotide diversity (π). Nucleotide diversity of the viral population was computed using the following formula[72]:

$\pi = \frac{D}{D-1}\left\{1 - \left[p^2 + (1-p)^2\right]\right\}$ with D, the sequencing depth and p the frequency of the minority variant at each nucleotide site. For diallelic SNV, π ranges from 0 to 0.5 (both alleles at equal frequency). In the subsequent analyses, π was averaged over all polymorphic nucleotide sites of the DCV genome of each sample[73]. A site was considered polymorphic if at least one sample showed the presence of a nucleotide variant at said position of the DCV genome. The $\log_{10}$-transformed site-averaged π values were then compared between fly genotypes (orthogonal factor), biological replicates (orthogonal factor), passages (continuous variable) and genomic regions (orthogonal factor) and their interactions using a GLM. The significance of each term in the model was evaluated using a likelihood ratio test that follows a χ^2 probability distribution.

Estimation of relative mutational fitness effects. We have followed the classic population genetics method described in Hartl and Clark[43]. In short, let $x_l(t)$ be the frequency of a mutant allele (SNP) at genomic position l and passage t and, therefore, $1 - x_l(t)$ the frequency of the wild-type allele. It holds that $\log\frac{x_l(t)}{1-x_l(t)} = \log\frac{x_l(0)}{1-x_l(0)} + t\log(1 - s_l)$, where s_l is the selection coefficient of the mutant relative to the wild-type allele at locus l. Selection coefficients calculated this way have units of inverse time (per passage in our case). This equation was fitted to the time-series data of each locus l shown in Fig. 3 by least squares regression, obtaining an estimate of s_l and its s.e.m.

Haplotype inference was done using two different statistical approaches. First, by assessing the similarity between temporal dynamics of all possible pairs of loci. To this end, Pearson partial correlation coefficients (controlling for passages) were computed and their significance level corrected for multiple tests of the same null hypothesis using Benjamini and Hochberg[74] FDR method. Correlation coefficient matrices were visualized as heatmaps in which more similar alleles were clustered together. Second, we confirmed the results from the first method using the longitudinal variant allele frequency factorization problem (LVAFFP) method as implemented in CALDER[75]. LVAFFP generates spanning trees of a directed graph constructed from the variant allele frequencies. The output of CALDER was used as input of TimeScape[76] to generate the Muller plots that illustrate the ancestry of mutations and haplotypes along the evolution experiment (Fig. 3).

Statistical analyses described in this section have been done with R v.4.0.2 in RStudio v.1.3.1073.

Reporting Summary. Further information on research design is available in the Nature Research Reporting Summary linked to this article.

Data availability

All raw data from high-throughput sequencing were deposited to NCBI BioProjects under accession number PRJNA782868. Source data are provided with this paper.

Code availability

Scripts are provided in Supplementary Data 1.

Received: 19 May 2021; Accepted: 14 December 2021;
Published online: 10 March 2022

References

1. Morgan, A. D. & Koskella, B. in *Genetics and Evolution of Infectious Diseases* (ed. Tibayrenc, M.) 115–140 (Elsevier, 2017).
2. Daugherty, M. D. & Malik, H. S. Rules of engagement: molecular insights from host–virus arms races. *Annu. Rev. Genet.* **46**, 677–700 (2012).
3. Barreiro, L. B. & Quintana-Murci, L. From evolutionary genetics to human immunology: how selection shapes host defence genes. *Nat. Rev. Genet.* **11**, 17–30 (2010).
4. Thompson, J. N. & Burdon, J. J. Gene-for-gene coevolution between plants and parasites. **360**, 121–125 (1992).
5. Buckling, A. & Rainey, P. B. Antagonistic coevolution between a bacterium and a bacteriophage. *Proc. Biol. Sci.* **269**, 931–936 (2002).
6. Masri, L. et al. Host–pathogen coevolution: the selective advantage of *Bacillus thuringiensis* virulence and its Cry toxin genes. *PLoS Biol.* **13**, e1002169 (2015).
7. Obbard, D. J., Gordon, K. H. J., Buck, A. H. & Jiggins, F. M. The evolution of RNAi as a defence against viruses and transposable elements. *Philos. Trans. R. Soc. B* **364**, 99–115 (2009).
8. Lazzaro, B. P. Natural selection on the *Drosophila* antimicrobial immune system. *Curr. Opin. Microbiol.* **11**, 284–289 (2008).
9. Lazzaro, B. P. Molecular population genetics of inducible antibacterial peptide genes in *Drosophila melanogaster*. *Mol. Biol. Evol.* **20**, 914–923 (2003).
10. Sackton, T. B. et al. Dynamic evolution of the innate immune system in *Drosophila*. *Nat. Genet.* **39**, 1461–1468 (2007).
11. Brackney, D. E., Beane, J. E. & Ebel, G. D. RNAi targeting of West Nile virus in mosquito midguts promotes virus diversification. *PLoS Pathog.* **5**, e1000502 (2009).
12. Lin, S.-S. et al. Molecular evolution of a viral non-coding sequence under the selective pressure of amiRNA-mediated silencing. *PLoS Pathog.* **5**, e1000312 (2009).
13. Lafforgue, G. et al. Tempo and mode of plant RNA virus escape from RNA interference-mediated resistance. *J. Virol.* **85**, 9686–9695 (2011).
14. Martínez, F. et al. Ultradeep sequencing analysis of population dynamics of virus escape mutants in RNAi-mediated resistant plants. *Mol. Biol. Evol.* **29**, 3297–3307 (2012).
15. Das, A. T. et al. Human immunodeficiency virus type 1 escapes from RNA interference-mediated inhibition. *J. Virol.* **78**, 2601–2605 (2004).
16. Gitlin, L., Stone, J. K. & Andino, R. Poliovirus escape from RNA interference: short interfering RNA-target recognition and implications for therapeutic approaches. *J. Virol.* **79**, 1027–1035 (2005).
17. Mondotte, J. A. & Saleh, M.-C. Antiviral immune response and the route of infection in *Drosophila melanogaster*. *Adv. Virus Res.* **100**, 247–278 (2017).
18. Swevers, L., Liu, J. & Smagghe, G. Defense mechanisms against viral infection in Drosophila: RNAi and non-RNAi. *Viruses* **10**, 230 (2018).
19. Galiana-Arnoux, D., Dostert, C., Schneemann, A., Hoffmann, J. A. & Imler, J.-L. Essential function in vivo for Dicer-2 in host defense against RNA viruses in *Drosophila*. *Nat. Immunol.* **7**, 590–597 (2006).
20. van Rij, R. P. et al. The RNA silencing endonuclease Argonaute 2 mediates specific antiviral immunity in *Drosophila melanogaster*. *Genes Dev.* **20**, 2985–2995 (2006).

21. Wang, X.-H. et al. RNA interference directs innate immunity against viruses in adult *Drosophila*. *Science* **312**, 452–454 (2006).
22. Zambon, R. A., Vakharia, V. N. & Wu, L. P. RNAi is an antiviral immune response against a dsRNA virus in *Drosophila melanogaster*. *Cell. Microbiol.* **8**, 880–889 (2006).
23. Costa, A., Jan, E., Sarnow, P. & Schneider, D. The Imd pathway is involved in antiviral immune responses in *Drosophila*. *PLoS ONE* **4**, e7436 (2009).
24. Sansone, C. L. et al. Microbiota-dependent priming of antiviral intestinal immunity in *Drosophila*. *Cell Host Microbe* **18**, 571–581 (2015).
25. Ferreira, Á. G. et al. The Toll–Dorsal pathway is required for resistance to viral oral infection in *Drosophila*. *PLoS Pathog.* **10**, e1004507 (2014).
26. Zambon, R. A., Nandakumar, M., Vakharia, V. N. & Wu, L. P. The Toll pathway is important for an antiviral response in *Drosophila*. *Proc. Natl Acad. Sci. USA* **102**, 7257–7262 (2005).
27. Dostert, C. et al. The Jak-STAT signaling pathway is required but not sufficient for the antiviral response of *Drosophila*. *Nat. Immunol.* **6**, 946–953 (2005).
28. Merkling, S. H. et al. The epigenetic regulator G9a mediates tolerance to RNA virus infection in *Drosophila*. *PLoS Pathog.* **11**, e1004692 (2015).
29. Christian, P. D. & Johnson, K. N. The novel genome organization of the insect picorna-like virus *Drosophila* C virus suggests this virus belongs to a previously undescribed virus family. *J. Gen. Virol.* **79**, 191–203 (1998).
30. Jousset, F. X. & Plus, N. Study of the vertical transmission and horizontal transmission of *Drosophila melanogaster* and *Drosophila immigrans* picornavirus (author's translation). *Ann. Microbiol.* **126**, 231–249 (1975).
31. Mondotte, J. A. et al. Immune priming and clearance of orally acquired RNA viruses in *Drosophila*. *Nat. Microbiol.* **3**, 1394–1403 (2018).
32. Torri, A., Mongelli, V., Mondotte, J. A. & Saleh, M.-C. Viral infection and stress affect protein levels of Dicer 2 and Argonaute 2 in *Drosophila melanogaster*. *Front. Immunol.* **11**, 362 (2020).
33. Deddouche, S. et al. The DExD/H-box helicase Dicer-2 mediates the induction of antiviral activity in *Drosophila*. *Nat. Immunol.* **9**, 1425–1432 (2008).
34. Gomariz-Zilber, E., Jeune, B. & Thomas-Orillard, M. Limiting conditions of the horizontal transmission of the *Drosophila* C virus in its host (*D. melanogaster*). *Acta Oecol.* **19**, 125–137 (1998).
35. Stevanovic, A. L. & Johnson, K. N. Infectivity of *Drosophila* C virus following oral delivery in *Drosophila* larvae. *J. Gen. Virol.* **96**, 1490–1496 (2015).
36. Royet, J. Epithelial homeostasis and the underlying molecular mechanisms in the gut of the insect model *Drosophila melanogaster*. *Cell. Mol. Life Sci.* **68**, 3651–3660 (2011).
37. Buchon, N., Broderick, N. A., Poidevin, M., Pradervand, S. & Lemaitre, B. *Drosophila* intestinal response to bacterial infection: activation of host defense and stem cell proliferation. *Cell Host Microbe* **5**, 200–211 (2009).
38. Buchon, N., Broderick, N. A., Chakrabarti, S. & Lemaitre, B. Invasive and indigenous microbiota impact intestinal stem cell activity through multiple pathways in *Drosophila*. *Genes Dev.* **23**, 2333–2344 (2009).
39. Buchon, N., Broderick, N. A., Kuraishi, T. & Lemaitre, B. *Drosophila* EGFR pathway coordinates stem cell proliferation and gut remodeling following infection. *BMC Biol.* **8**, 152 (2010).
40. Xu, J. et al. ERK signaling couples nutrient status to antiviral defense in the insect gut. *Proc. Natl Acad. Sci. USA* **110**, 15025–15030 (2013).
41. Lauring, A. S. & Andino, R. Quasispecies theory and the behavior of RNA viruses. *PLoS Pathog.* **6**, e1001005 (2010).
42. Isakov, O. et al. Deep sequencing analysis of viral infection and evolution allows rapid and detailed characterization of viral mutant spectrum. *Bioinformatics* **31**, 2141–2150 (2015).
43. Hartl, D. L. & Clark, A. G. *Principles of Population Genetics* 4th edn (Sinauer Associates, 2006).
44. Travisano, M., Mongold, J. A., Bennett, A. F. & Lenski, R. E. Experimental tests of the roles of adaptation, chance, and history in evolution. *Science* **267**, 87–90 (1995).
45. Desai, M. M. & Fisher, D. S. Beneficial mutation–selection balance and the effect of linkage on positive selection. *Genetics* **176**, 1759–1798 (2007).
46. Miralles, R. Clonal interference and the evolution of RNA viruses. *Science* **285**, 1745–1747 (1999).
47. Miralles, R., Moya, A. & Elena, S. F. Diminishing returns of population size in the rate of RNA virus adaptation. *J. Virol.* **74**, 3566–3571 (2000).
48. Pepin, K. M. & Wichman, H. A. Experimental evolution and genome sequencing reveal variation in levels of clonal interference in large populations of bacteriophage φX174. *BMC Evol. Biol.* **8**, 85 (2008).
49. Navarro, R., Ambrós, S., Martínez, F. & Elena, S. F. Diminishing returns of inoculum size on the rate of a plant RNA virus evolution. *Europhys. Lett.* **120**, 38001 (2017).
50. Pandit, A. & de Boer, R. J. Reliable reconstruction of HIV-1 whole genome haplotypes reveals clonal interference and genetic hitchhiking among immune escape variants. *Retrovirology* **11**, 56 (2014).
51. Strelkowa, N. & Lässig, M. Clonal interference in the evolution of influenza. *Genetics* **192**, 671–682 (2012).
52. Gerrish, P. J. & Lenski, R. E. in *Mutation and Evolution* (eds Woodruff, R. C. & Thompson, J. N.) 127–144 (Springer, 1998).
53. Held, T., Klemmer, D. & Lässig, M. Survival of the simplest in microbial evolution. *Nat. Commun.* **10**, 2472 (2019).
54. Novella, I. S., Zárate, S., Metzgar, D. & Ebendick-Corpus, B. E. Positive selection of synonymous mutations in vesicular stomatitis virus. *J. Mol. Biol.* **342**, 1415–1421 (2004).
55. Zanini, F. & Neher, R. A. Quantifying selection against synonymous mutations in HIV-1 env evolution. *J. Virol.* **87**, 11843–11850 (2013).
56. Martínez, M. A., Jordan-Paiz, A., Franco, S. & Nevot, M. Synonymous virus genome recoding as a tool to impact viral fitness. *Trends Microbiol.* **24**, 134–147 (2016).
57. Kieft, J. S., Zhou, K., Jubin, R. & Doudna, J. A. Mechanism of ribosome recruitment by hepatitis C IRES RNA. *RNA* **7**, 194–206 (2001).
58. Zhang, L. et al. lncRNA sensing of a viral suppressor of RNAi activates non-canonical innate immune signaling in *Drosophila*. *Cell Host Microbe* **27**, 115–128 (2020).
59. Navarro, R. et al. Defects in plant immunity modulate the rates and patterns of RNA virus evolution. Preprint at *bioRxiv* https://doi.org/10.1101/2020.10.13.337402 (2021).
60. Merkling, S. H. & van Rij, R. P. Analysis of resistance and tolerance to virus infection in *Drosophila*. *Nat. Protoc.* **10**, 1084–1097 (2015).
61. Lee, Y. S. et al. Distinct roles for *Drosophila* Dicer-1 and Dicer-2 in the siRNA/miRNA silencing pathways. *Cell* **117**, 69–81 (2004).
62. Okamura, K. Distinct roles for Argonaute proteins in small RNA-directed RNA cleavage pathways. *Genes Dev.* **18**, 1655–1666 (2004).
63. Levashina, E. A., Ohresser, S., Lemaitre, B. & Imler, J. L. Two distinct pathways can control expression of the gene encoding the *Drosophila* antimicrobial peptide metchnikowin. *J. Mol. Biol.* **278**, 515–527 (1998).
64. Rutschmann, S. et al. The Rel protein DIF mediates the antifungal but not the antibacterial host defense in *Drosophila*. *Immunity* **12**, 569–580 (2000).
65. Hedengren, M. et al. Relish, a central factor in the control of humoral but not cellular immunity in *Drosophila*. *Mol. Cell* **4**, 827–837 (1999).
66. Díaz-Benjumea, F. J. & García-Bellido, A. Behaviour of cells mutant for an EGF receptor homologue of *Drosophila* in genetic mosaics. *Proc. Biol. Sci.* **242**, 36–44 (1990).
67. Reed, L. J. & Muench, H. A simple method of estimating fifty percent endpoints. *Am. J. Epidemiol.* **27**, 493–497 (1938).
68. Hothorn, T., Bretz, F. & Westfall, P. Simultaneous inference in general parametric models. *Biom. J.* **50**, 346–363 (2008).
69. Fox, J. & Weisberg S. *An R Companion to Applied Regression* 3rd edn (Sage, 2019).
70. Lenth, R. V. et al. Estimated Marginal Means, aka Least-Squares Means. R package version 1.5.5 (2021).
71. Wickham, H. et al. Welcome to the Tidyverse. *J. Open Source Softw.* **4**, 1686 (2019).
72. Cornman, R. S. et al. Population-genomic variation within RNA viruses of the western honey bee, Apis mellifera, inferred from deep sequencing. *BMC Genomics* **14**, 154 (2013).
73. Lequime, S., Fontaine, A., Ar Gouilh, M., Moltini-Conclois, I. & Lambrechts, L. Genetic drift, purifying selection and vector genotype shape Dengue virus intra-host genetic diversity in mosquitoes. *PLoS Genet.* **12**, e1006111 (2016).
74. Benjamini, Y. & Hochberg, Y. Controlling the false discovery rate: a practical and powerful approach to multiple testing. *J. R. Stat. Soc. B* **57**, 289–300 (1995).
75. Myers, M. A., Satas, G. & Raphael, B. J. CALDER: inferring phylogenetic trees from longitudinal tumor samples. *Cell Syst.* **8**, 514–522 (2019).
76. Smith, M. A. et al. E-scapescape: interactive visualization of single-cell phylogenetics and cancer evolution. *Nat. Methods* **14**, 549–550 (2017).

Acknowledgements

We thank members of the Saleh Lab, M. Vignuzzi and J. Pfeiffer for fruitful discussions. We thank C. Meignin for Rel^{E20} and $Vago^{\Delta M10}$ flies. This work was supported by the European Research Council (FP7/2013–2019 ERC CoG 615220) and the French Government's Investissement d'Avenir programme, Laboratoire d'Excellence Integrative Biology of Emerging Infectious Diseases (grant no. ANR-10-LABX-62-IBEID) to M.-C.S. Work in S.F.E.'s laboratory was supported by grant nos BFU2015-65037-P and PID2019-103998GB-I00 (Spain Agencia Estatal de Investigación—FEDER) and PROMETEU2019/012 (Generalitat Valenciana).

Author contributions

V.M. and M.-C.S. conceived the study. V.M., M.-C.S., A.K. and L.Q.-M. established the experimental design. V.M., V.G., H.B and J.N. performed the investigations. S.L. and S.F.E. performed the formal analyses. V.M., S.F.E. and M.-C.S. wrote the paper and acquired funding.

Competing interests
The authors declare no competing interests.

Additional information
Extended data is available for this paper at https://doi.org/10.1038/s41559-022-01697-z.

Supplementary information The online version contains supplementary material available at https://doi.org/10.1038/s41559-022-01697-z.

Correspondence and requests for materials should be addressed to Santiago F. Elena or Maria-Carla Saleh.

Peer review information *Nature Ecology & Evolution* thanks Guan-Zhu Han and the other, anonymous, reviewer(s) for their contribution to the peer review of this work. Peer reviewer reports are available.

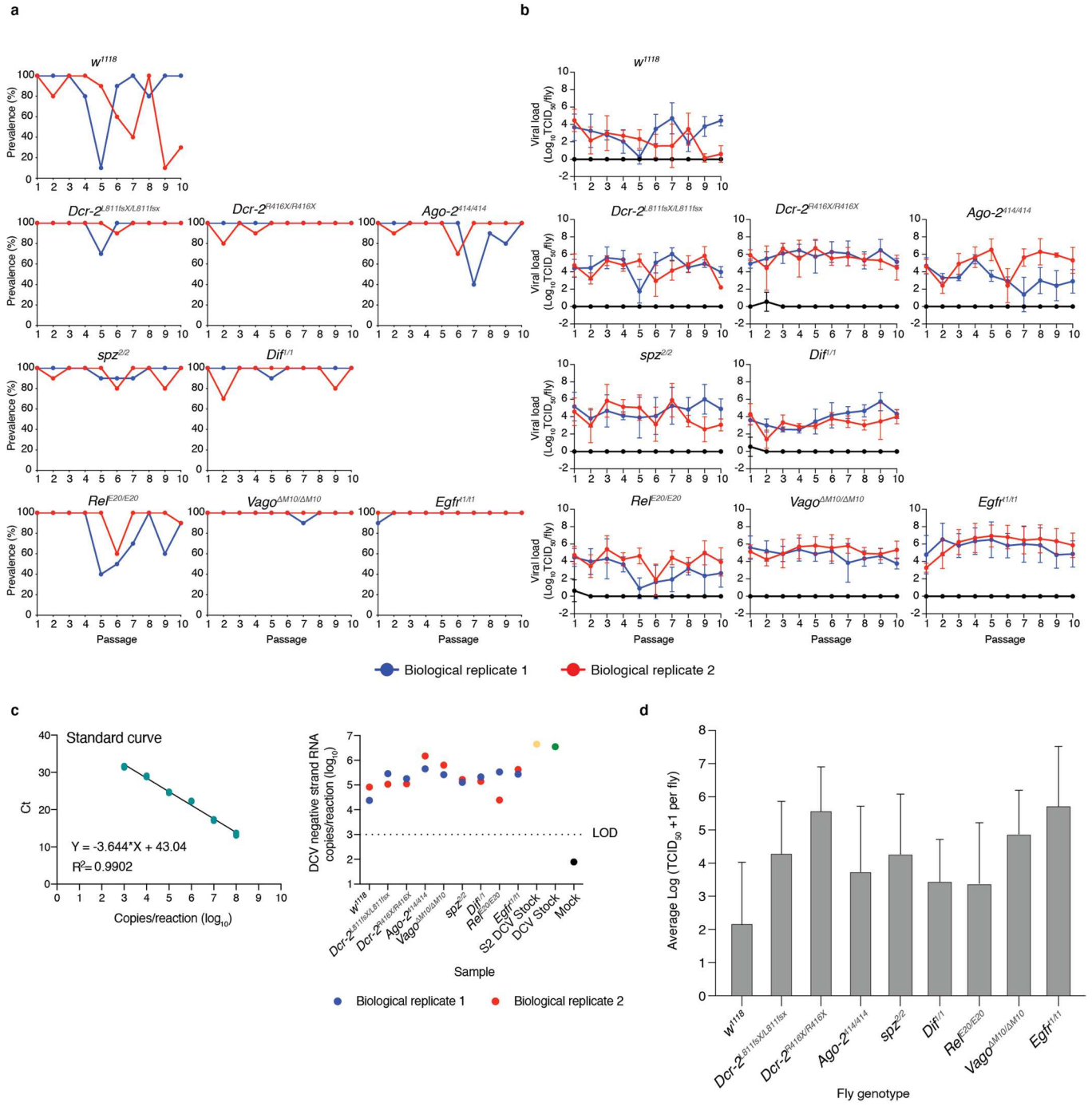

Extended Data Fig. 1 | Viral load and prevalence across the DCV evolution experiment. Viral load of 10 individual flies coming from DCV inoculated cages and four individual flies coming from mock inoculated cages was determined by $TCID_{50}$. **a)** Prevalence, calculated as the percentage of flies positive by $TCID_{50}$. **b)** Viral load determined by $TCID_{50}$ in each genotype across the 10 DCV passages. **c)** DCV replication assessed by negative-strand RT-qPCR. Left panel: standard curve produced from a tenfold dilution series over a range from 10^8 to 10^3 copies per reaction of in vitro transcribed RNA corresponding to a portion of the full-length negative-strand DCV RNA (slope = −3.644, $R^2 = 0.990$, efficiency = 88.25%). Right panel: amount of negative-strand DCV RNA present in the viral stocks produced from each fly genotype in P10, S2 DCV stock and DCV stock. Mock-infected flies were added as controls. LOD: Limit of detection of DCV negative stranded RNA. **d)** Average viral loads per individual fly of each genotype estimated from the GLM fitted to the data shown in panel b. Error bars represent ±1 SD.

	Condition	mean $\log_{10}$ (π) per site	SE	d.f.	asymp.LCL	asymp.UCL	Group
Full length genome, all viral passages	*w*^{1118}	0.0005	0.0001	Inf	0.0003	0.0009	1
	Dif$^{1/1}$	0.0007	0.0002	Inf	0.0004	0.0013	12
	Dcr-2$^{L811fsX/L811fsX}$	0.0011	0.0002	Inf	0.0006	0.0019	123
	Rel$^{E20/20}$	0.0014	0.0003	Inf	0.0008	0.0025	23
	spz$^{2/2}$	0.0015	0.0003	Inf	0.0009	0.0027	234
	Dcr-2$^{R416X/R416X}$	0.0017	0.0003	Inf	0.0009	0.0029	234
	Ago-2$^{414/414}$	0.0023	0.0005	Inf	0.0013	0.0041	34
	Egfr$^{1/t1}$	0.0036	0.0007	Inf	0.0020	0.0063	4
	Vago$^{DM10/DM10}$	0.0036	0.0007	Inf	0.0021	0.0063	4
All fly genotype, all viral passages	3'UTR	$1.98{\cdot}10^{-05}$	$2.44{\cdot}10^{-06}$	Inf	$1.46{\cdot}10^{-05}$	$2.70{\cdot}10^{-05}$	1
	5'UTR IRES	0.0001	$1.25{\cdot}10^{-05}$	Inf	0.0001	0.0002	2
	ORF1	0.0004	$3.68{\cdot}10^{-05}$	Inf	0.0004	0.0005	3
	ORF2	0.0006	$4.91{\cdot}10^{-05}$	Inf	0.0005	0.0007	3
Full length DCV genome, *P = 5*	*w*^{1118}	0.0004	0.0002	10	0.0001	0.0023	12
	Rel$^{E20/20}$	0.0007	0.0003	10	0.0001	0.0040	12
	Dif$^{1/1}$	0.0011	0.0005	10	0.0002	0.0064	12
	spz$^{2/2}$	0.0014	0.0007	10	0.0003	0.0080	12
	Ago-2$^{414/414}$	0.0015	0.0007	10	0.0003	0.0082	12
	Dcr-2$^{R416X/R416X}$	0.0016	0.0007	10	0.0003	0.0088	12
	Dcr-2$^{L811fsX/L811fsX}$	0.0018	0.0008	10	0.0003	0.0099	12
	Egfr$^{1/t1}$	0.0021	0.0010	10	0.0004	0.0117	12
	Vago$^{DM10/DM10}$	0.0041	0.0019	10	0.0007	0.0228	12
	DCV stock R1	0.0120	0.0057	10	0.0022	0.0667	2
	DCV stock R2	0.0110	0.0052	10	0.0020	0.0612	2
Full length DCV genome, *P = 10*	*Dif*$^{1/1}$	0.0003	0.0001	10	0.0001	0.0015	1
	spz$^{2/2}$	0.0006	0.0002	10	0.0001	0.0026	1
	w^{1118}	0.0007	0.0003	10	0.0002	0.0032	1
	Rel$^{E20/20}$	0.0008	0.0003	10	0.0002	0.0036	12
	Dcr-2$^{L811fsX/L811fsX}$	0.0011	0.0004	10	0.0003	0.0046	123
	Vago$^{DM10/DM10}$	0.0019	0.0007	10	0.0004	0.0080	123
	Egfr$^{1/t1}$	0.0020	0.0008	10	0.0005	0.0085	123
	Dcr-2$^{R416X/R416X}$	0.0023	0.0009	10	0.0005	0.0099	123
	Ago-2$^{414/414}$	0.0023	0.0009	10	0.0005	0.0099	123
	DCV stock R2	0.0110	0.0044	10	0.0026	0.0472	23
	DCV stock R1	0.0120	0.0048	10	0.0028	0.0514	3

Extended Data Fig. 2 | Grouping of DCV population swarms by similarity and increasing nucleotide diversity (π). Viral nucleotide diversity (π) was determined in each condition and grouped using a *post hoc* Bonferroni test based on the pairwise comparisons from Supplementary Table 1. SE: standard error. asymp.LCL: asymptomatic lower confidence level; asymp.UCL: asymptomatic upper confidence level.

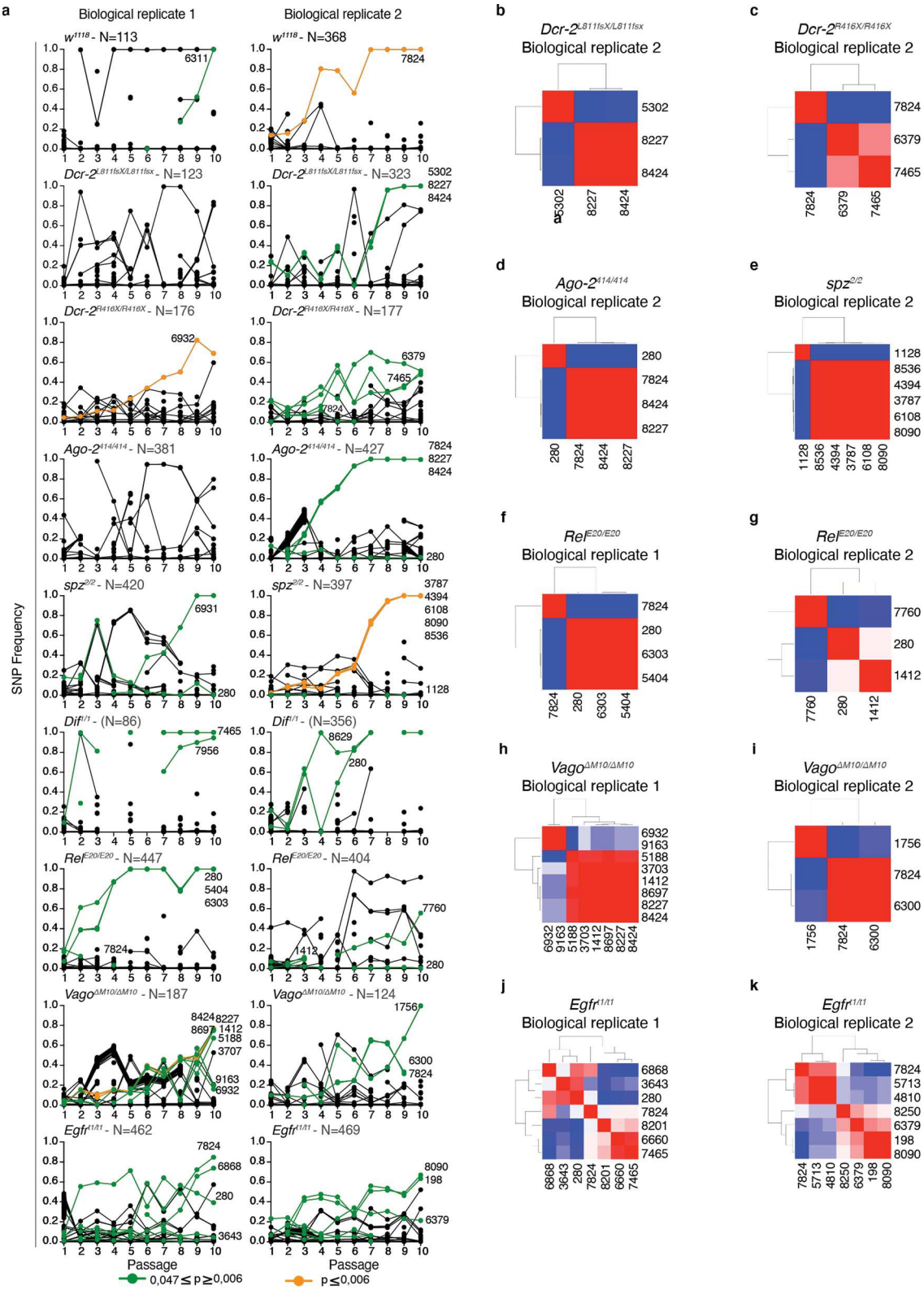

Extended Data Fig. 3 | Evolution of DCV variants. a) Trajectories of DCV variants across passages, *N*: total number of SPNs found above the estimated frequency threshold (≥ 0.0028). Trajectories of viral variants found significant after FDR correction are show in green ($p \leq 0.006$) and yellow ($0{,}047 \leq p \leq 0.006$) (based on data from Table 2). **b)** to **k)** Heatmaps showing the Pearson correlation coefficients between mutations' frequencies along evolutionary time, ranging from blue, where no linkage between the SNPs was found, to red, where the SNPs were linked in a same viral haplotype.

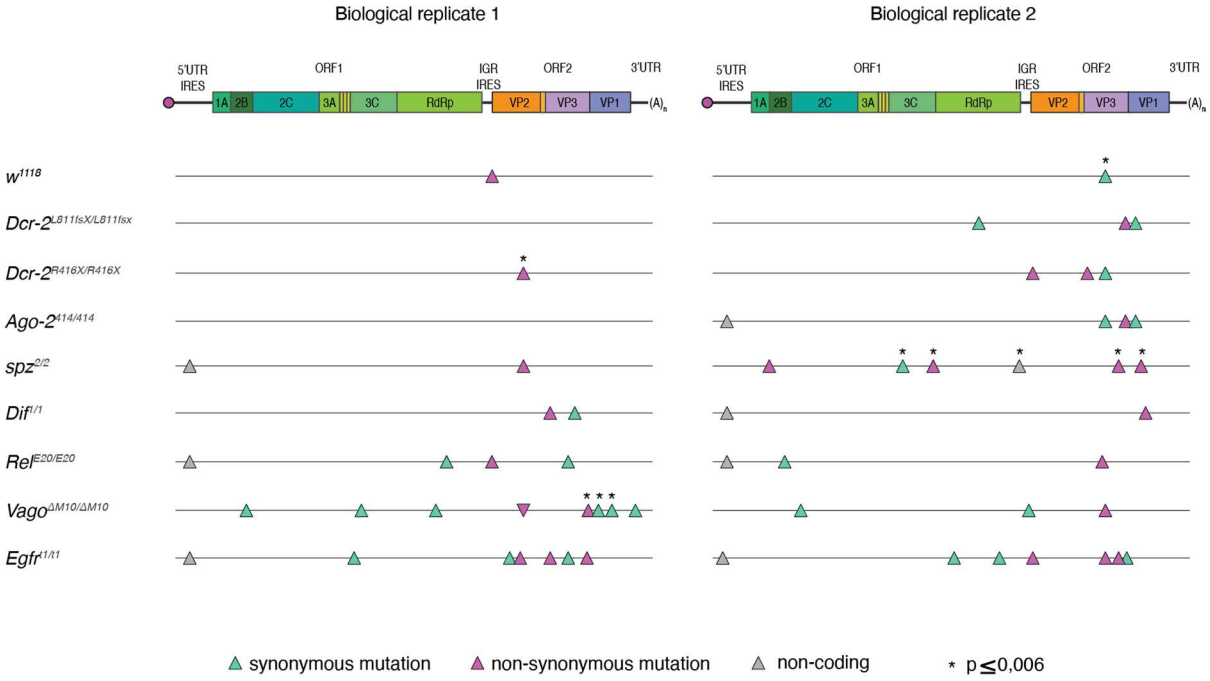

Extended Data Fig. 4 | SNPs on the DCV genome with significant estimates of fitness effects. Green triangles represent synonymous mutations, pink triangles non-synonymous mutations and grey triangles mutations in non-coding sequences. Cases significant after FDR correction ($p \leq 0.006$) are marked with an asterisk (based on data from Table 2).

nature portfolio

Corresponding author(s): Maria Carla Saleh

Last updated by author(s): Dec 13, 2021

Reporting Summary

Nature Portfolio wishes to improve the reproducibility of the work that we publish. This form provides structure for consistency and transparency in reporting. For further information on Nature Portfolio policies, see our Editorial Policies and the Editorial Policy Checklist.

Statistics

For all statistical analyses, confirm that the following items are present in the figure legend, table legend, main text, or Methods section.

n/a	Confirmed	
☐	☒	The exact sample size (*n*) for each experimental group/condition, given as a discrete number and unit of measurement
☐	☒	A statement on whether measurements were taken from distinct samples or whether the same sample was measured repeatedly
☐	☒	The statistical test(s) used AND whether they are one- or two-sided *Only common tests should be described solely by name; describe more complex techniques in the Methods section.*
☐	☒	A description of all covariates tested
☐	☒	A description of any assumptions or corrections, such as tests of normality and adjustment for multiple comparisons
☐	☒	A full description of the statistical parameters including central tendency (e.g. means) or other basic estimates (e.g. regression coefficient) AND variation (e.g. standard deviation) or associated estimates of uncertainty (e.g. confidence intervals)
☐	☒	For null hypothesis testing, the test statistic (e.g. *F*, *t*, *r*) with confidence intervals, effect sizes, degrees of freedom and *P* value noted *Give P values as exact values whenever suitable.*
☒	☐	For Bayesian analysis, information on the choice of priors and Markov chain Monte Carlo settings
☒	☐	For hierarchical and complex designs, identification of the appropriate level for tests and full reporting of outcomes
☐	☒	Estimates of effect sizes (e.g. Cohen's *d*, Pearson's *r*), indicating how they were calculated

Our web collection on statistics for biologists contains articles on many of the points above.

Software and code

Policy information about availability of computer code

Data collection	n/a
Data analysis	a) Comparison of survival curves was performed using a log-rank (Mantel–Cox) test and Prism v.8.4.3 (www.graphpad.com). b) Bioinformatics Analysis of NGS Libraries. VIVAN (http://www.vivanbioinfo.org) was used for SNPs detection. The quality of fastq files was assessed using graphs generated by FastQC (www.bioinformatics.babraham.ac.uk/projects/fastqc/). Using cutadapt (https://cutadapt.readthedocs.io/en/stable/), low-quality bases and adaptors were trimmed from each read. Codes for algorithms used in this study will be deposited in GitHub and are referenced in the manuscript. c) Variant frequency threshold, viral nucleotide diversity and estimation of relative mutational fitness effects were performed in R version 4.0.2 in RStudio version 1.3.1073.

For manuscripts utilizing custom algorithms or software that are central to the research but not yet described in published literature, software must be made available to editors and reviewers. We strongly encourage code deposition in a community repository (e.g. GitHub). See the Nature Portfolio guidelines for submitting code & software for further information.

Data

Policy information about availability of data

All manuscripts must include a data availability statement. This statement should provide the following information, where applicable:

- Accession codes, unique identifiers, or web links for publicly available datasets
- A description of any restrictions on data availability
- For clinical datasets or third party data, please ensure that the statement adheres to our policy

The data that support the findings of this study are available from the corresponding author upon request. In-house codes are also available at any time upon request to the authors.

Field-specific reporting

Please select the one below that is the best fit for your research. If you are not sure, read the appropriate sections before making your selection.

☒ Life sciences ☐ Behavioural & social sciences ☐ Ecological, evolutionary & environmental sciences

For a reference copy of the document with all sections, see nature.com/documents/nr-reporting-summary-flat.pdf

Life sciences study design

All studies must disclose on these points even when the disclosure is negative.

Sample size

a) DCV experimental evolution assay:
N = 500 5 to 6 days old wild type or mutant flies (males and females) were used in each viral passage. This procedure was repeated in 2 biological replicates for viral infected flies and in 1 biological replicate for mock inoculated flies.

i) To produce the NGS library total RNA was extracted from half of the population of infected flies from each fly genotype (approx. 250 flies) and each viral passages.
One NGS library was produced and sequenced per fly genotype/viral passage/biological replicate.
Four NGS libraries (2 biological and 2 technical replicates) were produced and sequenced from S2 DCV stock and DCV stock.

ii) To asses DCV virulence, infectious DCV stocks were produced from viral passages P = 1 and P = 10 using half of the population of infected flies from each fly genotype (approx. 250 flies). Survival curves were performed in w1118 flies. Two independent experiments with three biological replicates of 20 flies each were done per condition. Total number of flies per viral stock is indicated between brackets.

Biological Replicate 1
- Mock infected flies (235)
- S2 DCV stock (235)
- DCV stock (231)

Biological Replicate 1 - P = 1
- w1118 stock (119)
- Dcr-2 L811fsX/L811fsX stock (120)
- Dcr-2 R416X/R416X stock (118)
- Ago-2 414/414 stock (120)
- Spz 2/2 stock (119)
- Dif 1/1 stock (117)
- Rel E20/E20 stock (118)
- VagoΔ10/Δ10 stock (120)
- Egfr t1/t1 stock (119)

Biological Replicate 1 - P = 10
- w1118 stock (116)
- Dcr-2 L811fsX/L811fsX stock (114)
- Dcr-2 R416X/R416X stock (106)
- Ago-2 414/414 stock (115)
- Spz 2/2 stock (118)
- Dif 1/1 stock (117)
- Rel E20/E20 stock (110)
- VagoΔ10/Δ10 stock (108)
- Egfr t1/t1 stock (115)

Biological Replicate 2
- Mock infected flies (235)
- S2 DCV stock (225)
- DCV stock (233)

Biological Replicate 2 - P = 1

w1118 stock (119)
Dcr-2 L811fsX/L811fsX stock (119)
Dcr-2 R416X/R416X stock (119)
Ago-2 414/414 stock (118)
Spz 2/2 stock (119)
Dif 1/1 stock (119)
Rel E20/E20 stock (120)
VagoΔ10/Δ10 stock (120)
Egfr t1/t1 stock (115)

Biological Replicate 2 - P = 10
w1118 stock (104)
Dcr-2 L811fsX/L811fsX stock (105)
Dcr-2 R416X/R416X stock (110)
Ago-2 414/414 stock (111)
Spz 2/2 stock (102)
Dif 1/1 stock (98)
Rel E20/E20 stock (100)
VagoΔ10/Δ10 stock (94)
Egfr t1/t1 stock (98)

iii) To determine viral load and persistence during the course of the viral passages, viral load of 10 individual flies (5 males and 5 females) from DCV inoculated cages and four individual flies (2 males and 2 females) from mock inoculated cages was determined.

iv) To determine DCV replication, production of negative strand RNA was quantified using ssRT-qPCR according to the protocol published in DOI: 10.1016/j.jmb.2021.167308. The amount of negative strand DCV RNA present in the viral stocks produced from each fly genotype in P = 10, S2 DCV stock, and DCV stock was determined.

b) To characterize the newly produced back-crossed fly lines, survival curves were performed, the number of flies per condition is indicated between brackets. Two to three independent experiments with three biological replicates of 15 to 25 flies were done per condition.

DCV
w1118 (185); Dcr-2 L811fsX/L811fsX (182)
w1118 (191); Dcr-2 R416X/R416X (183)
w1118 (207); Ago-2 414/414 (161)
w1118 (131); Spz 2/2 (131)
w1118 (126); Dif 1/1 (132)
w1118 (194); Rel E20/E20 (180)
w1118 (132); VagoΔ10/Δ10 (131)
w1118 (131); Egfr t1/t1 (132)

Enterococcus faecalis
w1118 (83); Spz 2/2 (82)
w1118 (83); Dif 1/1 (84)
w1118 (83); Rel E20/E20 (86)

Erwinia carotovora
w1118 (90); Spz 2/2 (84)
w1118 (90); Dif 1/1 (87)
w1118 (90); Rel E20/E20 (71)

Data exclusions	No data were excluded from the analysis.
Replication	All attempts at replication were successful.
Randomization	For DCV evolution experiment and survival curves, synchronized flies reared in standard medium were randomly collected from different tubes and pooled, and the treatment was assigned.
Blinding	Blinding was not performed during the experiment, data acquisition, or analysis.

Reporting for specific materials, systems and methods

We require information from authors about some types of materials, experimental systems and methods used in many studies. Here, indicate whether each material, system or method listed is relevant to your study. If you are not sure if a list item applies to your research, read the appropriate section before selecting a response.

Materials & experimental systems

n/a	Involved in the study
☒	☐ Antibodies
☐	☒ Eukaryotic cell lines
☒	☐ Palaeontology and archaeology
☐	☒ Animals and other organisms
☒	☐ Human research participants
☒	☐ Clinical data
☒	☐ Dual use research of concern

Methods

n/a	Involved in the study
☒	☐ ChIP-seq
☒	☐ Flow cytometry
☒	☐ MRI-based neuroimaging

Eukaryotic cell lines

Policy information about cell lines

Cell line source(s)	Drosophila S2 cells, Life Technologies.
Authentication	None of the cell lines were authenticated.
Mycoplasma contamination	All cell lines used in this study tested negative for mycoplasma contamination.
Commonly misidentified lines (See ICLAC register)	*Name any commonly misidentified cell lines used in the study and provide a rationale for their use.*

Animals and other organisms

Policy information about studies involving animals; ARRIVE guidelines recommended for reporting animal research

Laboratory animals	Drosophila melanogaster (non ethical permission required).
Wild animals	n/a
Field-collected samples	n/a
Ethics oversight	n/a

Note that full information on the approval of the study protocol must also be provided in the manuscript.

nature portfolio

https://doi.org/10.1038/s41559-022-01697-z

Supplementary information

Innate immune pathways act synergistically to constrain RNA virus evolution in *Drosophila melanogaster*

In the format provided by the authors and unedited

Supplementary Information

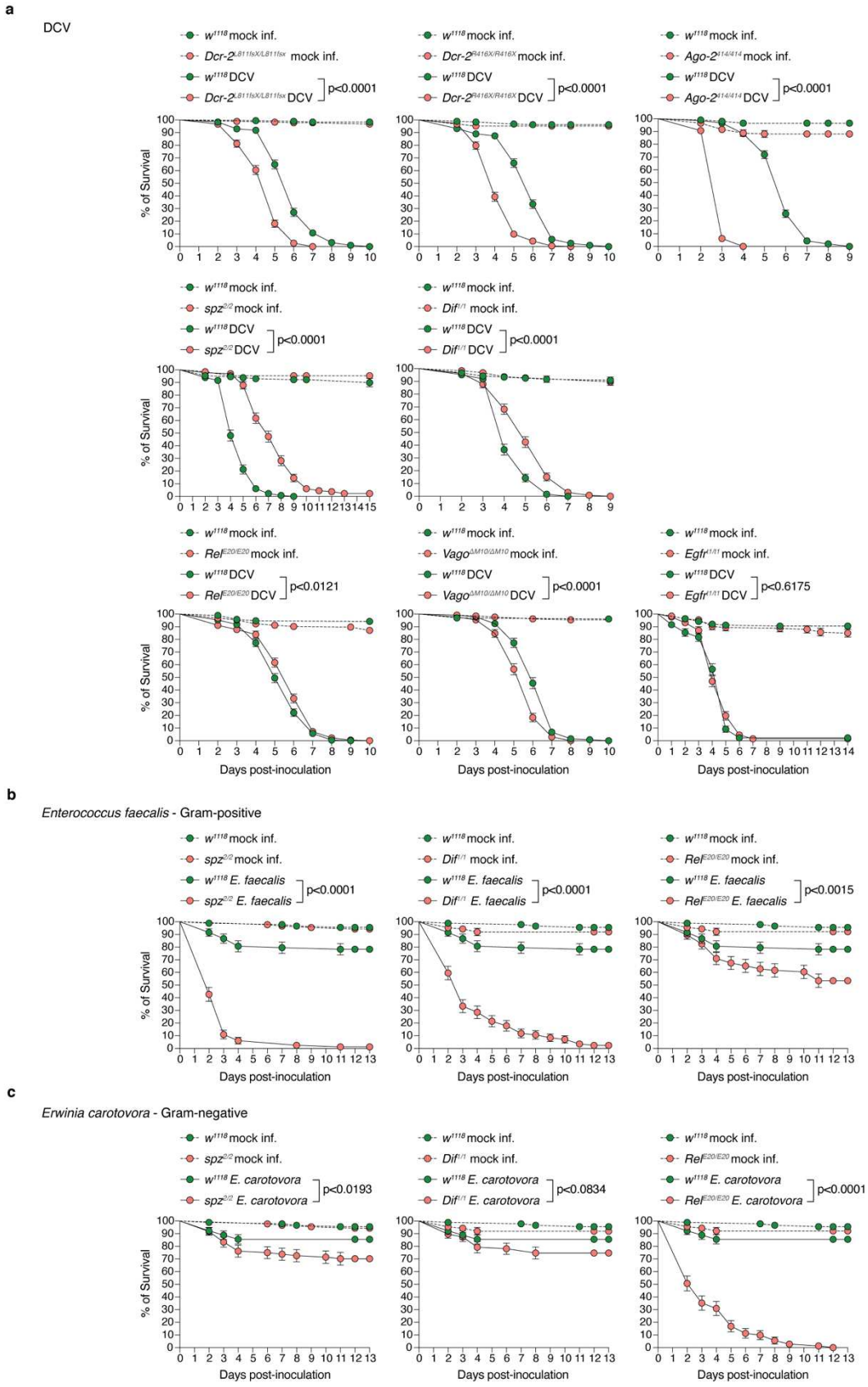

Supplementary Figure 1. Characterization of the newly produced innate immune backcrossed fly lines. Innate immune deficient fly lines backcrossed to w^{1118} genetic background were intrathoracically injected with **a)** 10 $TCID_{50}$ units of DCV, **b)** 50 nl of a suspension of optical density (OD) = 10 from *E. faecalis* (Gram + bacteria), and c) 50 nl of a suspension of OD = 200 from *E. carotovora carotovora 15* (Ecc15) (Gram + bacteria). After DCV and *E. faecalis* inoculation flies were kept at 25 °C and at 29 °C after Ecc15 inoculation. Survival was measured daily. Two independent experiments with three biological replicates of $N = 20$ flies each per condition were analyzed. Error bars indicate ±1 SEM; n.s., not significant. Survival curves were compared via log-rank (Mantel–Cox) tests.

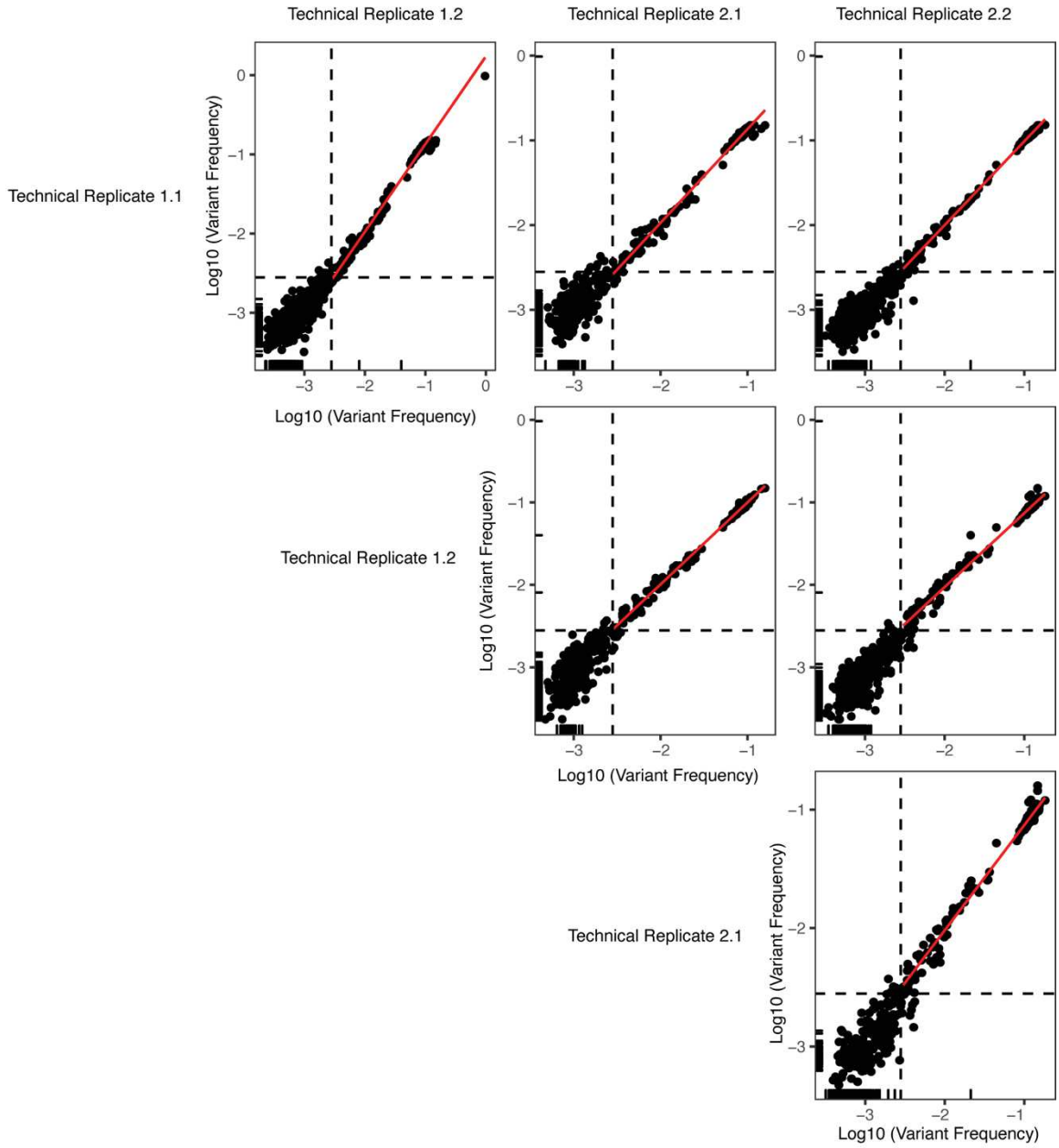

Supplementary Figure 2. Determination of NGS threshold error and mapping of sequenced derived from DCV starting stocks used. Pairwise correlation between variant frequency (log_{10}-transformed) in four technical sequencing replicates derived from S2 DCV stock. Dashed line represents the frequency threshold value used for subsequent analyses (0.0028). Red line represents the linear regression for variant frequency above the frequency threshold. Black ticks on axis represent missing variants in the other technical replicate under consideration.

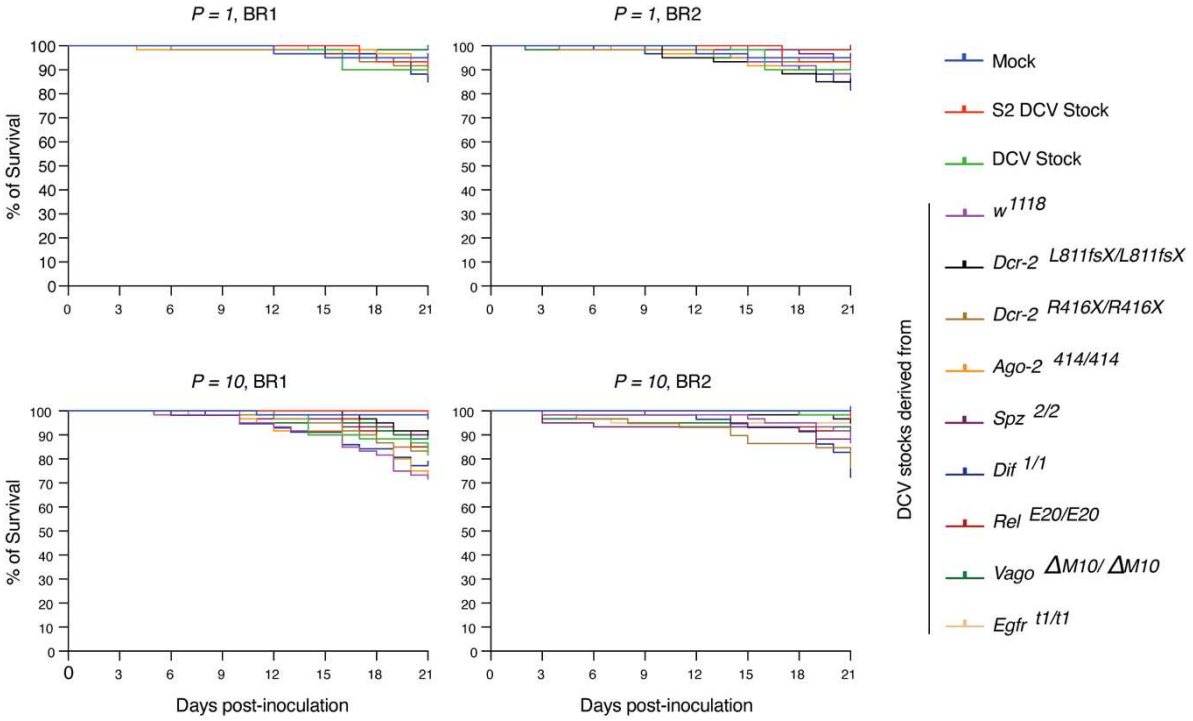

Supplementary Figure 3. Study of DCV virulence in *P* = 1 and *P* = 10 by oral infection. DCV infectious stocks were produced from viral passages *P* = 1 and *P* = 10 and from each fly genotype and biological replicate (BR1 and BR2). w^{1118} flies were orally infected with 10^6 $TCID_{50}$ units of DCV and survival was measured daily. Survival curves are the combination of two independent replicates, with three technical replicates each, of a total of at least *N* = 98 flies per treatment. Survival curves were compared via log-rank (Mantel–Cox) tests and no significant difference was found between the treatments.

Supplementary Table 1. Pairwise comparisons of DCV population diversity (Mean Log10 (π) per site). Pairwise comparison of viral nucleotide diversity between different conditions. For DCV stock, a total of four technical replicates were prepared and sequenced by pairs in 2 independent runs. For the purpose of this analysis each technical replicate derived from the same run was pooled, DCV stock R1 and R2 respectively. Statically significant p-values ($p < 0.05$) are in bold.

	Conditions compared	Estimate	SE	d.f.	*z.ratio*	*p*
Full length viral genome, all viral passages	*w*^{1118} - *Dcr-2*$^{L811fsX/L811fsX}$	0.3267	0.124	Inf	2.635	0.3026
	w^{1118} - *Dcr-2*$^{R416X/R416X}$	0.5088	0.124	Inf	4.103	**0.0015**
	w^{1118} - *Ago-2*$^{414/414}$	0.6573	0.124	Inf	5.301	**<0.0001**
	w^{1118} - *spz*$^{2/2}$	0.4750	0.124	Inf	3.831	**0.0046**
	w^{1118} - *Dif*$^{1/1}$	0.1372	0.130	Inf	1.059	1.0000
	w^{1118} - *Rel*$^{E20/20}$	0.4432	0.124	Inf	3.575	**0.0126**
	w^{1118} - *Vago*$^{DM10/DM10}$	0.8449	0.124	Inf	6.814	**<0.0001**
	w^{1118} - *Egfr*$^{t1/t1}$	0.8443	0.124	Inf	6.810	**<0.0001**
	Dcr-2$^{L811fsX/L811fsX}$ - *Dcr-2*$^{R416X/R416X}$	0.1820	0.124	Inf	1.468	1.0000
	Dcr-2$^{L811fsX/L811fsX}$ - *Ago-2*$^{414/414}$	0.3306	0.124	Inf	2.666	0.2762
	Dcr-2$^{L811fsX/L811fsX}$ - *spz*$^{2/2}$	-0.1483	0.124	Inf	-1.196	1.0000
	Dcr-2$^{L811fsX/L811fsX}$ - *Dif*$^{1/1}$	0.1895	0.130	Inf	1.462	1.0000
	Dcr-2$^{L811fsX/L811fsX}$ - *Rel*$^{E20/20}$	-0.1165	0.124	Inf	-0.939	1.0000
	Dcr-2$^{L811fsX/L811fsX}$ - *Vago*$^{DM10/DM10}$	-0.5181	0.124	Inf	-4.179	**0.0011**
	Dcr-2$^{L811fsX/L811fsX}$ - *Egfr*$^{t1/t1}$	-0.5175	0.124	Inf	-4.174	**0.0011**
	Dcr-2$^{R416X/R416X}$ - *Ago-2*$^{414/414}$	0.1485	0.124	Inf	1.198	1.0000
	Dcr-2$^{R416X/R416X}$ - *spz*$^{2/2}$	0.0337	0.124	Inf	0.272	1.0000
	Dcr-2$^{R416X/R416X}$ - *Dif*$^{1/1}$	0.3715	0.130	Inf	2.866	0.1497
	Dcr-2$^{R416X/R416X}$ - *Rel*$^{E20/20}$	0.0656	0.124	Inf	0.529	1.0000
	Dcr-2$^{R416X/R416X}$ - *Vago*$^{DM10/DM10}$	-0.3361	0.124	Inf	-2.711	0.2415
	Dcr-2$^{R416X/R416X}$ - *Egfr*$^{t1/t1}$	-0.3355	0.124	Inf	-2.706	0.2451
	Ago-2$^{414/414}$ - *spz*$^{2/2}$	0.1823	0.124	Inf	1.470	1.0000
	Ago-2$^{414/414}$ - *Dif*$^{1/1}$	0.5200	0.130	Inf	4.012	0.0022
	Ago-2$^{414/414}$ - *Rel*$^{E20/20}$	0.2141	0.124	Inf	1.727	1.0000
	Ago-2$^{414/414}$ - *Vago*$^{DM10/DM10}$	-0.1876	0.124	Inf	-1.513	1.0000
	Ago-2$^{414/414}$ - *Egfr*$^{t1/t1}$	-0.1870	0.124	Inf	-1.508	1.0000
	spz$^{2/2}$ - *Dif*$^{1/1}$	-0.3378	0.130	Inf	-2.606	0.3302
	spz$^{2/2}$ - *Rel*$^{E20/20}$	-0.0318	0.124	Inf	-0.257	1.0000
	spz$^{2/2}$ - *Vago*$^{DM10/DM10}$	-0.3699	0.124	Inf	-2.983	0.1027
	spz$^{2/2}$ - *Egfr*$^{t1/t1}$	0.3693	0.124	Inf	2.978	0.1043

	Dif$^{1/1}$ - *Rel*$^{E20/20}$	-0.3059	0.130	Inf	-2.360	0.6577
	Dif$^{1/1}$ - *Vago*$^{DM10/DM10}$	-0.7076	0.130	Inf	-5.459	**<0.0001**
	Dif$^{1/1}$ - *Egfr*$^{t1/t1}$	-0.7070	0.130	Inf	-5.454	**<0.0001**
	Rel$^{E20/20}$ - *Vago*$^{DM10/DM10}$	-0.4017	0.124	Inf	-3.240	**0.0431**
	Rel$^{E20/20}$ - *Egfr*$^{t1/t1}$	0.4011	0.124	Inf	3.235	**0.0438**
	Vago$^{DM10/DM10}$ - *Egfr*$^{t1/t1}$	-0.0006	0.124	Inf	-0.005	1.0000
All fly genotypes, all viral passages	5'UTR IRES - ORF1	-0.472	0.0512	Inf	-9.214	**<0.0001**
	5'UTR IRES - ORF2	-0.597	0.0512	Inf	-11.660	**<0.0001**
	ORF1 - ORF2	-0.125	0.0512	Inf	-2.450	0.0857
	3'UTR - ORF1	-1.348	0.0645	Inf	-20.915	**<0.0001**
	3'UTR - ORF2	-1.473	0.0645	Inf	-22.860	**<0.0001**
	3'UTR - 5'UTR IRES	-0.876	0.0645	Inf	-13.577	**<0.0001**
Full length DCV genome, P = *1*	*w*^{1118} - *Dcr-2*$^{L811fsX/L811fsX}$	-0.6811	0.605	10	-1.126	1.0000
	w^{1118} - *Dcr-2*$^{R416X/R416X}$	-0.5391	0.605	10	-0.891	1.0000
	w^{1118} - *Ago-2*$^{414/41}$	0.0175	0.605	10	0.029	1.0000
	w^{1118} - *spz*$^{2/2}$	0.0840	0.605	10	0.139	1.0000
	w^{1118} - *Dif*$^{1/1}$	0.0457	0.605	10	0.076	1.0000
	w^{1118} - *Rel*$^{E20/20}$	0.3081	0.605	10	0.509	1.0000
	w^{1118} - *Vago*$^{DM10/DM10}$	-0.5342	0.605	10	-0.883	1.0000
	w^{1118} - *Egfr*$^{t1/t1}$	0.2863	0.605	10	0.473	1.0000
	w^{1118} - DCV stock R1	0.3363	0.605	10	0.556	1.0000
	w^{1118} - DCV stock R2	0.2992	0.605	10	0.495	1.0000
	Dcr-2$^{L811fsX/L811fsX}$ - *Dcr-2*$^{R416X/R416X}$	0.1420	0.605	10	0.235	1.0000
	Dcr-2$^{L811fsX/L811fsX}$ - *Ago-2*$^{414/414}$	0.6986	0.605	10	1.155	1.0000
	Dcr-2$^{L811fsX/L811fsX}$ - *spz*$^{2/2}$	-0.7651	0.605	10	-1.265	1.0000
	Dcr-2$^{L811fsX/L811fsX}$ - *Dif*$^{1/1}$	-0.7268	0.605	10	-1.202	1.0000
	Dcr-2$^{L811fsX/L811fsX}$ - *Rel*$^{E20/20}$	-0.9892	0.605	10	-1.636	1.0000
	Dcr-2$^{L811fsX/L811fsX}$ - *Vago*$^{DM10/DM10}$	-0.1470	0.605	10	-0.243	1.0000
	Dcr-2$^{L811fsX/L811fsX}$ - *Egfr*$^{t1/t1}$	-0.9674	0.605	10	-1.600	1.0000
	Dcr-2$^{L811fsX/L811fsX}$ - DCV stock R1	-1.0174	0.605	10	-1.682	1.0000
	Dcr-2$^{L811fsX/L811fsX}$ - DCV stock R2	-0.9803	0.605	10	-1.621	1.0000
	Dcr-2$^{R416X/R416X}$ - *Ago-2*$^{414/414}$	0.5566	0.605	10	0.920	1.0000
	Dcr-2$^{R416X/R416X}$ - *spz*$^{2/2}$	-0.6230	0.605	10	-1.030	1.0000
	Dcr-2$^{R416X/R416X}$ - *Dif*$^{1/1}$	-0.5848	0.605	10	-0.967	1.0000
	Dcr-2$^{R416X/R416X}$ - *Rel*$^{E20/20}$	-0.8472	0.605	10	-1.401	1.0000
	Dcr-2$^{R416X/R416X}$ - *Vago*$^{DM10/DM10}$	-0.0049	0.605	10	-0.008	1.0000
	Dcr-2$^{R416X/R416X}$ - *Egfr*$^{t1/t1}$	-0.8253	0.605	10	-1.365	1.0000
	Dcr-2$^{R416X/R416X}$ - DCV stock R1	-0.8754	0.605	10	-1.447	1.0000
	Dcr-2$^{R416X/R416X}$ - DCV stock R2	-0.8383	0.605	10	-1.386	1.0000
	Ago-2$^{414/414}$ - *spz*$^{2/2}$	-0.0665	0.605	10	-0.110	1.0000
	Ago-2$^{414/414}$ - *Dif*$^{1/1}$	-0.0282	0.605	10	-0.047	1.0000

	Ago-2$^{414/414}$ - *Rel$^{E20/20}$*	-0.2906	0.605	10	-0.481	1.0000
	Ago-2$^{414/414}$ - *Vago$^{DM10/DM10}$*	0.5517	0.605	10	0.912	1.0000
	Ago-2$^{414/414}$ - *Egfr$^{t1/t1}$*	-0.2688	0.605	10	-0.444	1.0000
	Ago-2$^{414/414}$ - DCV stock R1	-0.3188	0.605	10	-0.527	1.0000
	Ago-2$^{414/414}$ - DCV stock R2	-0.2817	0.605	10	-0.466	1.0000
	spz$^{2/2}$ - *Dif$^{1/1}$*	-0.0383	0.605	10	-0.063	1.0000
	spz$^{2/2}$ - *Rel$^{E20/20}$*	0.2242	0.605	10	0.371	1.0000
	spz$^{2/2}$ - *Vago$^{DM10/DM10}$*	0.6181	0.605	10	1.022	1.0000
	spz$^{2/2}$ - *Egfr$^{t1/t1}$*	0.2023	0.605	10	0.335	1.0000
	spz$^{2/2}$ - DCV stock R1	0.2523	0.605	10	0.417	1.0000
	spz$^{2/2}$ - DCV stock R2	0.2152	0.605	10	0.356	1.0000
	Dif$^{1/1}$ - *Rel$^{E20/20}$*	-0.2624	0.605	10	-0.434	1.0000
	Dif$^{1/1}$ - *Vago$^{DM10/DM10}$*	0.5799	0.605	10	0.959	1.0000
	Dif$^{1/1}$ - *Egfr$^{t1/t1}$*	-0.2406	0.605	10	-0.398	1.0000
	Dif$^{1/1}$ - DCV stock R1	-0.2906	0.605	10	-0.481	1.0000
	Dif$^{1/1}$ - DCV stock R2	-0.2535	0.605	10	-0.419	1.0000
	Rel$^{E20/20}$ - *Vago$^{DM10/DM10}$*	0.8423	0.605	10	1.393	1.0000
	Rel$^{E20/20}$ - *Egfr$^{t1/t1}$*	-0.0219	0.605	10	-0.036	1.0000
	Rel$^{E20/20}$ - DCV stock R1	0.0282	0.605	10	0.047	1.0000
	Rel$^{E20/20}$ - DCV stock R2	-0.0089	0.605	10	-0.015	1.0000
	Vago$^{DM10/DM10}$ - *Egfr$^{t1/t1}$*	0.8204	0.605	10	1.357	1.0000
	Vago$^{DM10/DM10}$ - DCV Stock R1	0.8705	0.605	10	1.439	1.0000
	Vago$^{DM10/DM10}$ - DCV stock R2	0.8333	0.605	10	1.378	1.0000
	Egfr$^{t1/t1}$ - DCV stock R1	-0.0500	0.605	10	-0.083	1.0000
	Egfr$^{t1/t1}$ - DCV stock R2	-0.0129	0.605	10	-0.021	1.0000
	DCV stock R1 - DCV stock R2	0.0371	0.605	10	0.061	1.0000
Full length DCV genome, *P = 5*	*w^{1118}* - *Dcr-2$^{L811fsX/L811fsX}$*	0.6418	0.29	10	2.217	1.0000
	w^{1118} - *Dcr-2$^{R416X/R416X}$*	0.5894	0.29	10	2.036	1.0000
	w^{1118} - *Ago-2$^{414/41}$*	0.5614	0.29	10	1.939	1.0000
	w^{1118} - *spz$^{2/2}$*	0.5482	0.29	10	1.894	1.0000
	w^{1118} - *Dif$^{1/1}$*	0.4524	0.29	10	1.563	1.0000
	w^{1118} - *Rel$^{E20/20}$*	0.2449	0.29	10	0.846	1.0000
	w^{1118} - *Vago$^{DM10/DM10}$*	1.0051	0.29	10	3.471	0.3303
	w^{1118} - *Egfr$^{t1/t1}$*	0.7169	0.29	10	2.476	1.0000
	w^{1118} - DCV stock R1	1.4714	0.29	10	5.082	**0.0262**
	w^{1118} - DCV stock R2	1.4343	0.29	10	4.954	**0.0316**
	Dcr-2$^{L811fsX/L811fsX}$ - *Dcr-2$^{R416X/R416X}$*	-0.0524	0.29	10	-0.181	1.0000
	Dcr-2$^{L811fsX/L811fsX}$ - *Ago-2$^{414/414}$*	-0.0804	0.29	10	-0.278	1.0000
	Dcr-2$^{L811fsX/L811fsX}$ - *spz$^{2/2}$*	0.0936	0.29	10	0.323	1.0000
	Dcr-2$^{L811fsX/L811fsX}$ - *Dif$^{1/1}$*	0.1894	0.29	10	0.654	1.0000

Dcr-2$^{L811fsX/L811fsX}$ - *Rel*$^{E20/20}$	0.3969	0.29	10	1.371	1.0000
Dcr-2$^{L811fsX/L811fsX}$ - *Vago*$^{DM10/DM10}$	-0.3633	0.29	10	-1.255	1.0000
Dcr-2$^{L811fsX/L811fsX}$ - *Egfr*$^{t1/t1}$	-0.0751	0.29	10	-0.259	1.0000
Dcr-2$^{L811fsX/L811fsX}$ - DCV stock R1	-0.8296	0.29	10	-2.865	0.9240
Dcr-2$^{L811fsX/L811fsX}$ - DCV stock R2	-0.7925	0.29	10	-2.737	1.0000
Dcr-2$^{R416X/R416X}$ - *Ago-2*$^{414/414}$	-0.0280	0.29	10	-0.097	1.0000
Dcr-2$^{R416X/R416X}$ - *spz*$^{2/2}$	0.0411	0.29	10	0.142	1.0000
Dcr-2$^{R416X/R416X}$ - *Dif*$^{1/1}$	0.1369	0.29	10	0.473	1.0000
Dcr-2$^{R416X/R416X}$ - *Rel*$^{E20/20}$	0.3444	0.29	10	1.190	1.0000
Dcr-2$^{R416X/R416X}$ - *Vago*$^{DM10/DM10}$	-0.4157	0.29	10	-1.436	1.0000
Dcr-2$^{R416X/R416X}$ - *Egfr*$^{t1/t1}$	-0.1275	0.29	10	-0.441	1.0000
Dcr-2$^{R416X/R416X}$ - DCV stock R1	-0.8821	0.29	10	-3.047	0.6778
Dcr-2$^{R416X/R416X}$ - DCV stock R2	-0.8449	0.29	10	-2.918	0.8440
Ago-2$^{414/414}$ - *spz*$^{2/2}$	0.0132	0.29	10	0.045	1.0000
Ago-2$^{414/414}$ - *Dif*$^{1/1}$	0.1090	0.29	10	0.376	1.0000
Ago-2$^{414/414}$ - *Rel*$^{E20/20}$	0.3165	0.29	10	1.093	1.0000
Ago-2$^{414/414}$ - *Vago*$^{DM10/DM10}$	-0.4437	0.29	10	-1.532	1.0000
Ago-2$^{414/414}$ - *Egfr*$^{t1/t1}$	-0.1555	0.29	10	-0.537	1.0000
Ago-2$^{414/414}$ - DCV stock R1	-0.9100	0.29	10	-3.143	0.5750
Ago-2$^{414/414}$ - DCV stock R2	-0.8729	0.29	10	-3.015	0.7155
spz$^{2/2}$ - *Dif*$^{1/1}$	-0.0958	0.29	10	-0.331	1.0000
spz$^{2/2}$ - *Rel*$^{E20/20}$	-0.3033	0.29	10	-1.048	1.0000
spz$^{2/2}$ - *Vago*$^{DM10/DM10}$	-0.4569	0.29	10	-1.578	1.0000
spz$^{2/2}$ - *Egfr*$^{t1/t1}$	0.1687	0.29	10	0.583	1.0000
spz$^{2/2}$ - DCV stock R1	0.9232	0.29	10	3.189	0.5323
spz$^{2/2}$ - DCV stock R2	0.8861	0.29	10	3.060	0.6621
Dif$^{1/1}$ - *Rel*$^{E20/20}$	0.2075	0.29	10	0.717	1.0000
Dif$^{1/1}$ - *Vago*$^{DM10/DM10}$	-0.5527	0.29	10	-1.909	1.0000
Dif$^{1/1}$ - *Egfr*$^{t1/t1}$	-0.2645	0.29	10	-0.914	1.0000
Dif$^{1/1}$ - DCV stock R1	-1.0190	0.29	10	-3.520	0.3049
Dif$^{1/1}$ - DCV stock R2	-0.9819	0.29	10	-3.391	0.3779
Rel$^{E20/20}$ - *Vago*$^{DM10/DM10}$	-0.7602	0.29	10	-2.626	1.0000
Rel$^{E20/20}$ - *Egfr*$^{t1/t1}$	0.4720	0.29	10	1.630	1.0000
Rel$^{E20/20}$ - DCV stock R1	1.2265	0.29	10	4.236	0.0950
Rel$^{E20/20}$ - DCV stock R2	1.1894	0.29	10	4.108	0.1165
Vago$^{DM10/DM10}$ - *Egfr*$^{t1/t1}$	-0.2882	0.29	10	-0.995	1.0000
Vago$^{DM10/DM10}$ - DCV Stock R1	0.4663	0.29	10	1.611	1.0000
Vago$^{DM10/DM10}$ - DCV stock R2	0.4292	0.29	10	1.482	1.0000
Egfr$^{t1/t1}$ - DCV stock R1	-0.7545	0.29	10	-2.606	1.0000
Egfr$^{t1/t1}$ - DCV stock R2	-0.7174	0.29	10	-2.478	1.0000
DCV stock R1 - DCV stock R2	0.0371	0.29	10	0.128	1.0000

Full length DCV genome, *P = 10*	*w*^{1118} - *Dcr-2*$^{L811fsX/L811fsX}$	0.1642	0.246	10	0.668	1.0000
	w^{1118} - *Dcr-2*$^{R416X/R416X}$	0.4977	0.246	10	2.026	1.0000
	w^{1118} - *Ago-2*$^{414/41}$	0.4988	0.246	10	2.031	1.0000
	w^{1118} - *spz*$^{2/2}$	-0.0775	0.246	10	-0.316	1.0000
	w^{1118} - *Dif*$^{1/1}$	-0.3342	0.246	10	-1.361	1.0000
	w^{1118} - *Rel*$^{E20/20}$	0.0590	0.246	10	0.240	1.0000
	w^{1118} - *Vago*$^{DM10/DM10}$	0.4039	0.246	10	1.644	1.0000
	w^{1118} - *Egfr*$^{t1/t1}$	0.4290	0.246	10	1.746	1.0000
	w^{1118} - DCV stock R1	1.2133	0.246	10	4.940	**0.0323**
	w^{1118} - DCV stock R2	1.1762	0.246	10	4.788	**0.0405**
	Dcr-2$^{L811fsX/L811fsX}$ - *Dcr-2*$^{R416X/R416X}$	0.3335	0.246	10	1.358	1.0000
	Dcr-2$^{L811fsX/L811fsX}$ - *Ago-2*$^{414/414}$	0.3346	0.246	10	1.362	1.0000
	Dcr-2$^{L811fsX/L811fsX}$ - *spz*$^{2/2}$	0.2417	0.246	10	0.984	1.0000
	Dcr-2$^{L811fsX/L811fsX}$ - *Dif*$^{1/1}$	0.4984	0.246	10	2.029	1.0000
	Dcr-2$^{L811fsX/L811fsX}$ - *Rel*$^{E20/20}$	0.1052	0.246	10	0.428	1.0000
	Dcr-2$^{L811fsX/L811fsX}$ - *Vago*$^{DM10/DM10}$	-0.2397	0.246	10	-0.976	1.0000
	Dcr-2$^{L811fsX/L811fsX}$ - *Egfr*$^{t1/t1}$	-0.2648	0.246	10	-1.078	1.0000
	Dcr-2$^{L811fsX/L811fsX}$ - DCV stock R1	-1.0491	0.246	10	-4.271	0.0899
	Dcr-2$^{L811fsX/L811fsX}$ - DCV stock R2	-1.0120	0.246	10	-4.120	0.1142
	Dcr-2$^{R416X/R416X}$ - *Ago-2*$^{414/414}$	0.0011	0.246	10	0.004	1.0000
	Dcr-2$^{R416X/R416X}$ - *spz*$^{2/2}$	0.5752	0.246	10	2.342	1.0000
	Dcr-2$^{R416X/R416X}$ - *Dif*$^{1/1}$	0.8319	0.246	10	3.387	0.3806
	Dcr-2$^{R416X/R416X}$ - *Rel*$^{E20/20}$	0.4387	0.246	10	1.786	1.0000
	Dcr-2$^{R416X/R416X}$ - *Vago*$^{DM10/DM10}$	0.0939	0.246	10	0.382	1.0000
	Dcr-2$^{R416X/R416X}$ - *Egfr*$^{t1/t1}$	0.0688	0.246	10	0.280	1.0000
	Dcr-2$^{R416X/R416X}$ - DCV stock R1	-0.7156	0.246	10	-2.913	0.8512
	Dcr-2$^{R416X/R416X}$ - DCV stock R2	-0.6785	0.246	10	-2.762	1.0000
	Ago-2$^{414/414}$ - *spz*$^{2/2}$	0.5763	0.246	10	2.346	1.0000
	Ago-2$^{414/414}$ - *Dif*$^{1/1}$	0.8330	0.246	10	3.391	0.3778
	Ago-2$^{414/414}$ - *Rel*$^{E20/20}$	0.4398	0.246	10	1.791	1.0000
	Ago-2$^{414/414}$ - *Vago*$^{DM10/DM10}$	0.0950	0.246	10	0.387	1.0000
	Ago-2$^{414/414}$ - *Egfr*$^{t1/t1}$	0.0699	0.246	10	0.284	1.0000
	Ago-2$^{414/414}$ - DCV stock R1	-0.7145	0.246	10	-2.909	0.8578
	Ago-2$^{414/414}$ - DCV stock R2	-0.6774	0.246	10	-2.758	1.0000
	spz$^{2/2}$ - *Dif*$^{1/1}$	-0.2567	0.246	10	-1.045	1.0000
	spz$^{2/2}$ - *Rel*$^{E20/20}$	0.1365	0.246	10	0.556	1.0000
	spz$^{2/2}$ - *Vago*$^{DM10/DM10}$	-0.4814	0.246	10	-1.960	1.0000
	spz$^{2/2}$ - *Egfr*$^{t1/t1}$	0.5065	0.246	10	2.062	1.0000
	spz$^{2/2}$ - DCV stock R1	1.2908	0.246	10	5.255	**0.0204**
	spz$^{2/2}$ - DCV stock R2	1.2537	0.246	10	5.104	**0.0254**
	Dif$^{1/1}$ - *Rel*$^{E20/20}$	-0.3932	0.246	10	-1.601	1.0000

Dif$^{1/1}$ - *Vago*$^{DM10/DM10}$	-0.7381	0.246	10	-3.005	0.7278
Dif$^{1/1}$ - *Egfr*$^{t1/t1}$	-0.7632	0.246	10	-3.107	0.6114
Dif$^{1/1}$ - DCV stock R1	-1.5475	0.246	10	-6.300	**0.0049**
Dif$^{1/1}$ - DCV stock R2	-1.5104	0.246	10	-6.149	**0.0060**
Rel$^{E20/20}$ - *Vago*$^{DM10/DM10}$	-0.3449	0.246	10	-1.404	1.0000
Rel$^{E20/20}$ - *Egfr*$^{t1/t1}$	0.3700	0.246	10	1.506	1.0000
Rel$^{E20/20}$ - DCV stock R1	1.1543	0.246	10	4.699	**0.0463**
Rel$^{E20/20}$ - DCV stock R2	1.1172	0.246	10	4.548	0.0584
Vago$^{DM10/DM10}$ - *Egfr*$^{t1/t1}$	0.0251	0.246	10	0.102	1.0000
Vago$^{DM10/DM10}$ - DCV Stock R1	0.8094	0.246	10	3.295	0.4441
Vago$^{DM10/DM10}$ - DCV stock R2	0.7723	0.246	10	3.144	0.5739
Egfr$^{t1/t1}$ - DCV stock R1	-0.7843	0.246	10	-3.193	0.5281
Egfr$^{t1/t1}$ - DCV stock R2	-0.7472	0.246	10	-3.042	0.6830
DCV stock R1 - DCV stock R2	0.0371	0.246	10	0.151	1.0000

Supplementary Table 2. Statistical analysis of the fly survival curves from Figure 5a. The table shows the number of flies used in the experiments, the median survival of the flies in each experimental setting and the *p* values of pairwise comparisons of the survival curves determined by Log-rank (Mantel–Cox) tests. These analyses were performed using GraphPad Prism 8.4.3.

Viral Passage 1 – Biological replicate 1

Viral stock Origin	Nr. of flies	Median survival	Viral stock Origin										
			Mock	**S2 DCV stock**	**DCV stock**	***w*^{1118}**	***Dcr-2*$^{L811fsX/L811fsX}$**	***Dcr-2*$^{R416X/R416X}$**	***Ago-2*$^{414/414}$**	***spz*$^{2/2}$**	***Dif*$^{1/1}$**	***Rel*$^{E20/20}$**	***Vago*$^{DM10/DM10}$**
Mock	235	Und.											
S2 DCV stock	235	5	<0,0001										
DCV stock	231	6	<0,0001 ****	<0,0001 ****									
***w*^{1118}**	119	5	<0,0001 ****	0,1152 ns	<0,0001 ****								
***Dcr-2*$^{L811fsX/L811fsX}$**	120	4	<0,0001 ****	<0,0001 ****	<0,0001 ****	<0,0001 ****							
***Dcr-2*$^{R416X/R416X}$**	118	5	<0,0001 ****	0,3054 ns	<0,0001 ****	0,6783 ns	<0,0001 ****						
***Ago-2*$^{414/414}$**	120	4	<0,0001 ****	<0,0001 ****	<0,0001 ****	<0,0001 ****	0,1412 ns	<0,0001 ****					
***spz*$^{2/2}$**	119	5	<0,0001 ****	0,2037 ns	<0,0001 ****	0,0007 ***	<0,0001 ****	0,0061 **	<0,0001 ****				
***Dif*$^{1/1}$**	117	5	<0,0001 ****	0,0888 ns	<0,0001 ****	0,8372 ns	<0,0001 ****	0,7587 ns	<0,0001 ****	0,0004 ***			
***Rel*$^{E20/20}$**	118	5	<0,0001 ****	<0,0001 ****	<0,0001 ****	0,0222 *	<0,0001 ****	0,0024 **	0,0007 ***	<0,0001 ****	0,0044 **		
***Vago*$^{DM10/DM10}$**	120	5	<0,0001 ****	0,0038 **	<0,0001 ****	0,3019 ns	<0,0001 ****	0,1366 ns	0,0004 ***	<0,0001 ****	0,1696 ns	0,3443 ns	
***Egfr*$^{1/1}$**	119	6	<0,0001 ****	<0,0001 ****	0,0002 ***	<0,0001 ****	<0,0001 ****	<0,0001 ****	<0,0001 ****	0,0038 **	<0,0001 ****	<0,0001 ****	<0,0001 ****

Viral Passage 10 – Biological replicate 1

Viral stock Origin	Nr. of flies	Median survival	Viral stock Origin										
			Mock	**S2 DCV stock**	**DCV stock**	***w*^{1118}**	***Dcr-2*$^{L811fsX/L811fsX}$**	***Dcr-2*$^{R416X/R416X}$**	***Ago-2*$^{414/414}$**	***spz*$^{2/2}$**	***Dif*$^{1/1}$**	***Rel*$^{E20/20}$**	***Vago*$^{DM10/DM10}$**
Mock	235	Und.											

S2 DCV stock	235	5	<0,0001											
DCV stock	231	6	<0,0001 ****	<0,0001 ****										
***w*^{1118}**	116	6	<0,0001 ****	0,3626 ns	<0,0001 ****									
***Dcr-2*$^{L811fsX/L811fsX}$**	114	6	<0,0001 ****	<0,0001 ****	0,0655 *ns*	<0,0001 ****								
***Dcr-2*$^{R416X/R416X}$**	106	6	<0,0001 ****	0,0008 ***	<0,0001 ****	0,0228 *	0,0029 **							
***Ago-2*$^{414/414}$**	115	6	<0,0001 ****	<0,0001 ****	0,5588 ns	<0,0001 ****	0,1497 ns	0,0003 ***						
***spz*$^{2/2}$**	118	5	<0,0001 ****	0,353 ns	<0,0001 ****	0,6788 ns	<0,0001 ****	0,004 **	<0,0001 ****					
***Dif*$^{1/1}$**	117	6	<0,0001 ****	0,0063 **	<0,0001 ****	0,1699 ns	<0,0001 ****	0,2717 ns	<0,0001 ****	0,0416 *				
***Rel*$^{E20/20}$**	110	6	<0,0001 ****	<0,0001 ****	0,0020 **	0,0027 **	0,2122 ns	0,2453 ns	0,0185 *	0,0014 **	0,0493 *			
***Vago*$^{DM10/DM10}$**	108	5	<0,0001 ****	0,0126 *	<0,0001 ****	0,147 ns	0,0003 ***	0,428 ns	<0,0001 ****	0,074 ns	0,9034 ns	0,066 ns		
***Egfr*$^{t1/t1}$**	115	6	<0,0001 ****	<0,0001 ****	0,8472 ns	<0,0001 ****	0,017 *	<0,0001 ****	0,607 ns	<0,0001 ****	<0,0001 ****	0,0011 **	<0,0001 ****	

Viral Passage 1 – Biological replicate 2

Viral stock Origin	Nr. of flies	**Median survival**	**Viral stock Origin**										
			Mock	**S2 DCV stock**	**DCV stock**	***w*^{1118}**	***Dcr-2*$^{L811fsX/L811fsX}$**	***Dcr-2*$^{R416X/R416X}$**	***Ago-2*$^{414/414}$**	***spz*$^{2/2}$**	***Dif*$^{1/1}$**	***Rel*$^{E20/20}$**	***Vago*$^{DM10/DM10}$**
Mock	235	Und.											
S2 DCV stock	225	5	<0,0001 ****										
DCV stock	233	6	<0,0001 ****	<0,0001 ****									
***w*^{1118}**	119	4	<0,0001 ****	<0,0001 ****	<0,0001 ****								
***Dcr-2*$^{L811fsX/L811fsX}$**	119	5	<0,0001 ****	0,0209 *	<0,0001 ****	0,0300 *							
***Dcr-2*$^{R416X/R416X}$**	119	5	<0,0001 ****	0,2219 ns	<0,0001 ****	<0,0001 ****	0,0012 **						
***Ago-2*$^{414/414}$**	118	4	<0,0001	<0,0001	<0,0001	0,3835	0,0025	<0,0001					

			****	****	****	ns	**	****					
***spz*$^{2/2}$**	119	5	<0,0001	0,2456	<0,0001	<0,0001	0,0011	0,9665	<0,0001				
			****	ns	****	****	**	ns	****				
***Dif*$^{1/1}$**	119	4	<0,0001	<0,0001	<0,0001	0,2122	0,3402	<0,0001	0,0329	<0,0001			
			****	****	****	ns	ns	****	*	****			
***Rel*$^{E20/20}$**	120	5	<0,0001	<0,0001	<0,0001	0,009	0,6047	0,0062	0,0005	0,005	0,1455		
			****	****	****	**	ns	**	***	**	ns		
***Vago*$^{DM10/DM10}$**	120	6	<0,0001	<0,0001	<0,0001	<0,0001	<0,0001	<0,0001	<0,0001	<0,0001	<0,0001	<0,0001	
			****	****	****	****	****	****	****	****	****	****	
***Egfr*$^{t1/t1}$**	115	5	<0,0001	0,1738	0,5815	<0,0001	0,0005	0,1995	<0,0001	0,1971	<0,0001	0,0016	0,0033
			****	ns	ns	****	***	ns	****	ns	****	**	**

Viral Passage 10 – Biological replicate 2

Viral stock Origin	**Nr. of flies**	**Median survival**	**Viral stock Origin**										
			Mock	**S2 DCV stock**	**DCV stock**	***w*^{1118}**	***Dcr-2*$^{L811fsX/L811fsX}$**	***Dcr-2*$^{R416X/R416X}$**	***Ago-2*$^{414/414}$**	***spz*$^{2/2}$**	***Dif*$^{1/1}$**	***Rel*$^{E20/20}$**	***Vago*$^{DM10/DM10}$**
Mock	235	Und.											
S2 DCV stock	225	5	<0,0001										
			****										
DCV stock	233	6	<0,0001	<0,0001									
			****	****									
***w*^{1118}**	104	5	<0,0001	0,0209	0,0083								
			****	*	**								
***Dcr-2*$^{L811fsX/L811fsX}$**	105	5	<0,0001	0,1381	0,0004	0,3873							
			****	ns	***	ns							
***Dcr-2*$^{R416X/R416X}$**	110	5	<0,0001	0,0011	0,0211	0,6294	0,1213						
			****	**	*	ns	ns						
***Ago-2*$^{414/414}$**	111	5	<0,0001	0,1376	0,0005	0,4395	0,9246	0,1763					
			****	ns	***	ns	ns	ns					
***spz*$^{2/2}$**	102	5	<0,0001	0,0003	0,2429	0,2615	0,0400	0,3852	0,0602				
			****	***	ns	ns	*	ns	ns				
***Dif*$^{1/1}$**	98	5	<0,0001	0,0979	0,0018	0,5727	0,698	0,3219	0,8399	0,1019			
			****	ns	**	ns	ns	ns	ns	ns			
***Rel*$^{E20/20}$**	100	5	<0,0001	0,0905	0,002	0,6142	0,7401	0,3066	0,7993	0,1219	0,9375		
			****	ns	**	ns	ns	ns	ns	ns	ns		
***Vago*$^{DM10/DM10}$**	94	5	<0,0001	0,0013	0,1121	0,3741	0,0779	0,5576	0,0992	0,8418	0,146	0,1781	
			****	**	ns	ns	ns	ns	ns	ns	ns	ns	
***Egfr*$^{t1/t1}$**	98	5	<0,0001	0,0297	0,0101	0,9411	0,4563	0,5765	0,5522	0,1878	0,7472	0,7471	0,3464
			****	*	*	ns	ns	ns	ns	ns	ns	ns	ns